AN ABSTRACT OF THE THESIS OF

FLOYD WILLIAM WOOD (Name) for the Master of Materials Science (Degree)

in Materials Science (Solids) (Major) presented on August 7, 1969 (Date)

Title: NEUTRON-INDUCED AUTORADIOGRAPHY OF LITHIA-SILICA MICROSPECIMENS: SPECIMEN PREPARATION AND PRELIMINARY ALPHA TRACKING

Abstract approved: Redacted for Privacy
Alan H. Robinson

Lithia-silica compositions between lithium disilicate and pure silica were explored theoretically and experimentally, with special emphasis on structural miscibility. Diffusion couples of vitreous materials were prepared and annealed. Best success in preparation was achieved by using electron-bombardment heating in vacuum to melt the less refractory glass and let it solidify around some of the more refractory material. Annealing was done with the protection of flowing argon at about 885° C for times up to 350.3 hours.

Diffusion profiles were measured by neutron-induced autoradiography, but before this could be done, it was necessary to establish practical conditions for using the technique, and to calibrate it for lithia-silica compositions. This was the first known application of its sort for the method of neutron-induced autoradiography, and

problems were encountered. This work represents a basis for improving several technical aspects.

Results of the work completed can be considered only tentative, but it is believed that evidence of a liquid-liquid miscibility gap was observed for the lithia-silica compositions studied. Furthermore, it is suspected that the bounds of the miscibility gap at about 885° C are near 7 and 20 mol percent lithia, and that related spinodal compositions are near 11 and 15 mol percent lithia. The values on the lithium disilicate side of the gap are in general agreement with previous determinations, but no prior experimental evidence concerning the silica side of the gap has been reported.

Both neutron-induced autoradiography and its application to basic investigation of the lithia-silica phase system were sufficiently promising to warrant repetition and extension of the work with improvements to increase confidence in the outcome.

Neutron-Induced Autoradiography of Lithia-Silica Microspecimens: Specimen Preparation and Preliminary Alpha Tracking

by

Floyd William Wood

A THESIS

submitted to

Oregon State University

in partial fulfillment of
the requirements for the
degree of

Master of Materials Science

June 1970

APPROVED:

Redacted for Privacy

Associate Professor of Nuclear Engineering

Redacted for Privacy

Head of Department of Mechanical and Nuclear Engineering

Redacted for Privacy

Dean of Graduate School

Date thesis is presented August 7, 1969

Typed by Muriel Davis for Floyd William Wood

ACKNOWLEDGMENT

This presentation is based on work done as a part of National Science Foundation Grant No. GK-2043, A Study of Light Element Miscibilities in Glass. All autoradiographic aspects of the work were done at the Radiation Center, Oregon State University. However, most of the specimen preparation and diffusion couple annealing were done in equipment located at the Albany Metallurgy Research Center of the U. S. Bureau of Mines. The Bureau's staff also contributed some previously prepared samples of appropriate glasses. Without this help, the work could not have been done, and the Bureau's contribution is deeply appreciated.

I am indebted to Dr. Alan H. Robinson, Associate Professor, and Charles R. Porter, Research Associate, of the Oregon State University Radiation Center, for guidance and assistance in all nuclear engineering aspects of the work, including autoradiography. Henry M. Harris, Jack I. Paige, and John E. Kelley of the Bureau of Mines' Albany Metallurgy Research Center supported me with materials, advice, and sympathy during early difficulties with materials preparation. I also had a useful telephone conversation with Dr. R. J. Charles of the General Electric Co. Research and Development Center. Of course, I also thank administrators of the Bureau of Mines' laboratory, especially H. Gordon Poole, Research Director, and Robert A. Beall, Coordinator of Metals Processing Projects, for their tolerance and interest.

TABLE OF CONTENTS

LIST OF FIGURES

LIST OF TABLES

NEUTRON-INDUCED AUTORADIOGRAPHY OF LITHIA-SILICA MICROSPECIMENS: SPECIMEN PREPARATION AND PRELIMINARY ALPHA TRACKING

INTRODUCTION

Objectives

In recent years, various methods have been developed to measure distributions of atoms at surfaces where diffusion, segregation, phase separation, deposition, corrosion, and similar events have occurred. Included are microprobe analysis, special electron diffraction techniques, low-angle x-ray scattering, secondary electron microscopy, Auger electron spectroscopy, and autoradiography. This presentation concerns the latter method which is especially useful for high-resolution matching of compositional differences with structural features. In past practice, the radiation involved has emanated from a naturally radioactive or activated component or tracer in the substance being examined. A photosensitive detector often has been used and special photographic emulsions have been developed for the purpose.

A new variation of autoradiography is based on alpha-particle ejection from certain light-element isotopes because of capture of thermal neutrons. Glasses, ceramics, metallic compounds, and alloys containing lithium or boron are especially amenable to the

technique. However, the method is still in its infancy, few guidelines are available for practical applications, and almost all aspects need further exploration and improvement. Accordingly, the work to be described here was done for two main purposes: (a) to evaluate the use of neutron-induced autoradiography in microscopic studies of selected ceramics and glasses, and specifically, (b) to investigate possible immiscibilities of silica-rich compositions in the lithia-silica pseudo-binary phase system. The lithia-silica combinations were formed by diffusion.

The Lithia-Silica System

The compositions of interest in this investigation lie between lithium disilicate, $Li_2O \cdot 2SiO_2$, and pure silica, SiO_2. In general, these two compounds will be treated as the terminal constituents of a pseudo-binary sub-system of the silica-rich lithia-silica phases. The sub-system is of the eutectic type as shown in Figure 1. Much about the phases involved has been discussed in scientific literature, and the features to be described below represent a composite interpretation and condensation of many publications (1, 2, 4, 6, 7, 8, 9, 10, 12, 13, 14, 15, 16, 17, 19, 20, 21, 22, 23, 24, 25, 26, 27, 29, 30, 31, 32, 33, 34). Some insight into complexities of the system can be gained by first considering the terminal constituents, silica and lithium disilicate, separately.

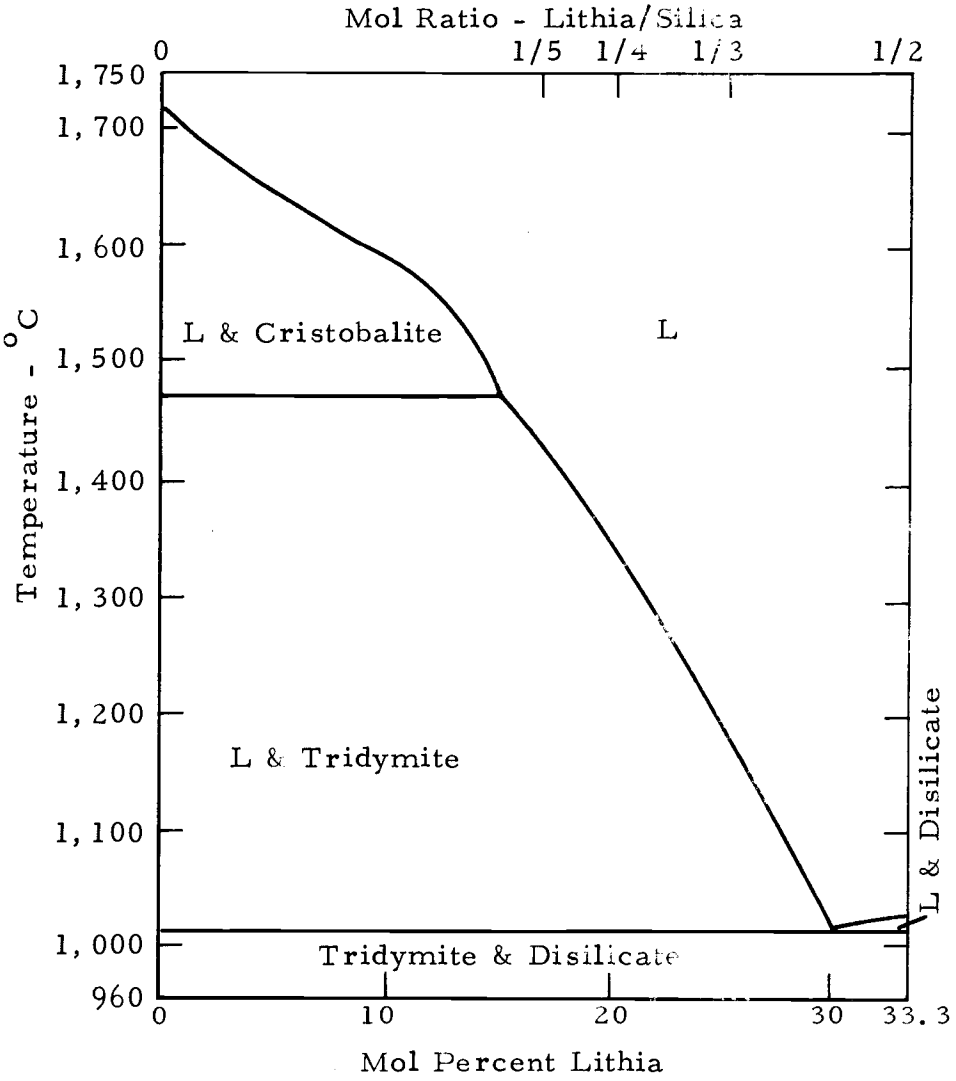

Figure 1. Equilibrium phases between silica and lithium disilicate.

Silica

Depending on how phases are defined and distinguished from each other, as many as 22 separate phases of silica have been identified, and there are a few others that have questionable existences. However, even in most mineralogical contexts, consideration of about ten phases is sufficient, and for purposes of this discussion the list may be restricted to an amorphous phase plus the high-temperature displacive polymorphs of three reconstructive crystal forms: quartz, tridymite, and cristobalite. At normal pressure, beta quartz is stable in the temperature range 573 to 867° C. It also can be heated in a metastable condition to its melting point near 1, 460° C. Beta tridymite is the stable form between 867 and 1, 470° C at one atmosphere of pressure, but it often is present as a metastable phase at tempatures down to about 163° C, and up to 1, 680° C, its melting point. Beta cristobalite, under normal pressure, is stable between 1, 470 and 1, 723° C, but it exists as a metastable phase between 272 and 1, 470° C. Normally, only liquid exists at temperatures above 1, 723° C. It is apparent that quartz, tridymite, and cristobalite can coexist in various degrees of stability over a rather broad temperature range. The metastable crystalline polymorphs are prevalent because the reconstructive transformations are extremely sluggish.

The sluggishness of crystallization also permits the formation

of a glassy phase or vitreous silica when liquid is cooled rapidly enough and in the absence of crystallizing catalysts. This is another metastable form that may achieve greater stability by devitrifying or crystallizing. Thermal devitrification is a time-at-temperature matter, and "devitrification temperatures" are rather imprecise and indefinite. In the case of pure vitreous silica, complete devitrification can be accomplished in about one hour at 1,600° C, about two hours at 1,500° C, or about three days at 1,200° C, and significant degrees of partial crystallization result in a few hours at 1,300° C or slightly less. However, these times and temperatures may be greatly altered by catalytic agents in the form of either energy or matter. Evidently, glassy silica almost always devitrifies by transforming first to cristobalite even if it subsequently transforms to another form (most likely tridymite).

Structurally, silica is more closely related to silicates than to most other oxides. Silica, like the silicates, is characterized by covalent silicon-oxygen atom groupings with a silicon atom tetrahedrally surrounded by four oxygen atoms. In pure silica, each of the oxygen atoms is shared between two tetrahedra of a three-dimensional network so that the stoichiometric requirements of a dioxide are satisfied. The polymorphic differences are due to different relative orientations and positions of silicon-oxygen tetrahedra, and to deviations from ideality of the tetrahedra themselves.

A few crystallographic details are listed in Table 1.

Table 1. The Three Principal High-Temperature Crystalline Polymorphs of Silica

Polymorph:	beta quartz	beta tridymite	beta cristobalite
Crystal System:	hexagonal	hexagonal	cubic
Symmetry:	622	6/mmm	23
Space Group:	#180 or 181, $P6_222$ or $P6_422$	#194, $P6_3/m2/m2/c$	#198, $P2_13$
Unit Cell:	3 Si, 6 O a = 5.0 A c = 5.47 A	4 Si, 8 O a = 5.04 A c = 8.24 A	8 Si, 16 O a = 7.14 A

Crystal structures of the three beta modifications may be visualized in terms of the tetrahedral silicon-oxygen units whose spatial distributions are specified by locations of the central silicon atoms. For example, the right-handed enantiomorph of beta quartz has silicon atoms at the following unit cell points: 1/2 0 0, 1/2 1/2 1/3, and 0 1/2 2/3. The beta tridymite and beta cristobalite structures are related to the wurtzite and zincblende structures of ZnS in the sense that the Si atoms of the former two structures occupy approximately the same unit cell positions as the Zn and S atoms of the latter two structures. Thus, the Si atoms in beta tridymite are located at 0 0 0, 0 0 7/16, 1/3 2/3 1/2, and 1/3 2/3 15/16, and the

Si atoms in beta cristobalite are at 0 0 0, 1/2 1/2 0, 1/2 0 1/2, 0 1/2 1/2, 1/4 1/4 1/4, 3/4 3/4 1/4, 1/4 3/4 3/4, and 3/4 1/4 3/4. In all three of the beta structures, oxygen atoms are ideally imagined to occupy sites midway between silicon atoms on a line connecting them, but in general, the oxygen sites actually are displaced slightly from the ideal positions. In either case, tetrahedral corners are shared. The silicon skeletons of the beta tridymite and cristobalite structures also may be viewed as corrugated-sheet arrangements. In the beta cristobalite, the successive layers are identical except for a translation normal to the direction in which the layers are stacked. In beta tridymite, however, the successive layers of Si atoms are related not only by a slight normal translation, but also by a two-fold rotation about the stacking direction.

Lithium Disilicate

Information about $Li_2O \cdot 2SiO_2$ as a separate phase is very scarce and somewhat uncertain. The room-temperature form appears to undergo a displacive transformation at about 937° C, then a reconstructive transformation at about 972° C. The melting range is about 1,028 to 1,033° C. Besides the crystalline forms there is a vitreous condition of metastable short-range order for lithium disilicate, just as there is for silica.

The low-temperature crystalline form of lithium disilicate has

a C-centered structure that is either monoclinic (with suggested parameters $a = 5.82$, $b = 14.66$, $c = 4.79$ A, and $\beta = 90^{\circ}$) or orthorhombic with probable space-group symmetry of Ccc2. At 937° C, the C-centering characteristic seems to be lost and the symmetry likely becomes primitive monoclinic. Above 972° C, a primitive orthorhombic symmetry is suspected, possibly Pcc2.

In the C-centered polymorph of lithium disilicate, silicon is coordinated by oxygen atoms in the familiar tetrahedral arrangement, and lithium is present as Li^{+} ions, also tetrahedrally coordinated by oxygen atoms. Each SiO_4 tetrahedron is associated with one other by means of a shared edge to form double units of composition Si_2O_6. The double units are each joined to others at corner points to form corrugated sheets of net stoichiometry Si_2O_5. The Li^{+} ions occupy tetrahedral interstices between the silicon-oxygen layers, coordinated by otherwise unshared oxygen atoms and resulting in the overall composition $Li_2Si_2O_5$ or $Li_2O \cdot 2SiO_2$. No similarly complete descriptions of the other polymorphs are yet possible.

Annealing of vitreous lithium disilicate at 460° C for 100 hours fails to cause any crystallization optically detectable at 600X magnification. Yet, a 50-hour treatment at 500° C produces a nicely devitrified product. Similar results can be obtained by a two-stage treatment for 15 hours each at 545° C and 800° C. The two-stage procedure is used because it has been observed that there is a high

risk of cracking unless special precautions are taken when lithium disilicate is heated above about 560° C.

Combinations of Silica and Lithium Disilicate

Silica and lithium disilicate can be combined in either their crystalline or vitreous forms, and it is well to discuss briefly some aspects of each type of combination. To differentiate between the general possibilities, the terms "crystalline solution" and "liquid miscibility" will be used.

According to a strict acceptance and literal interpretation of the phase diagram in Figure 1, there are no stable crystalline solutions in the composition range being considered. At equilibrium, only segregated combinations of the terminal phases, silica and lithium disilicate, should be expected, although they might be separated on an extremely fine scale. But actually, though they may be explainable as non-equilibrium situations, there is ample evidence that other types of combinations display considerable persistence.

One type of crystalline solution is the interstitial inclusion of Li^+ ions in silica. It may be significant to note that Li^+ is the only alkali-metal ion small enough (about 0.6 A diameter) to enter all three polymorphs interstitially. Na^+ and K^+ can do so in tridymite and cristobalite, but not in quartz. Of course, interstitial solutions of Li^+ ions, as such, in crystalline silica lack charge neutrality,

and they must be considered metastable. One way of achieving charge neutrality, hence greater stability, is to substitute a cation like Al^{3+}, of ionic valence three, for some of the Si^{4+}. This sort of an event is very undesirable for the purpose of investigating lithia-silica as a binary system. Another way would be to introduce the lithium as neutral atoms instead of ions. Li is about two and a half times as large as Li^{+}, but even so it is only slightly larger than K^{+}, so in principle, the neutral species should be able to enter the tridymite and cristobalite structures at least. However, the 2s valence electron of lithium is very weakly bound by an energy of about five electron volts. Therefore, as a result of lattice-potential interaction, Li tends to lose its valence electron which becomes a free electron. Thus, even when lithium is infused as neutral atoms, it exists in the structure as ions with their charges balanced by free electrons. But lithium combined in one way or another with oxygen is more readily available and easier to use as a source material for diffusion than elemental lithium.

Lithia is quite stable. Even at $1,500^{\circ}$ K, about 136 kcal/mol are still required for dissociation. Free lithium is not likely to be available from this source. The lithia molecule itself is almost twice as big as Li and nearly five times as big as Li^{+}, so penetration into the bulk of silica crystals by interstitial diffusion should be limited. But crystalline solutions containing at least up to five mol

percent of Li_2O in tridymite have been prepared regardless of expectations, and in any case, structural defects in silica should allow some diffusion of Li_2O, especially along crystallite boundaries. Lithia has a cubic anti-fluorite structure ($a \cong 4.6$ A) which is essentially a face-centered arrangement of oxygen atoms with a lithium atom inserted in each octant of the cubic cell. This should be reasonably compatible with either tridymite or cristobalite.

The bulky size of lithium disilicate molecules virtually precludes any expectation of interdiffusion by gross molecules. But the lithium in lithium disilicate exists as Li^+ ions, charge-compensated by free electrons, not unlike the situation in the crystalline solutions of Li^+ in SiO_2. So, an interaction seems possible between silica and lithium disilicate whereby Li^+ ions drift from the latter to the former. However, in such an event, the Li^+ would leave behind an unstable Si_2O_5 configuration and the interaction should not progress far unless there was a neutralizing back-diffusion of one Si^{4+} ion for every four departing Li^+ ions. Even this exchange should not proceed without restriction. Long before any compositional equilibrium could be reached, reconstructive changes probably would be required by the size disparity between a Si^{4+} ion (~ 0.4 A) and four Li^+ ions (~ 0.6 A each). The inability of a single structure to accommodate the alternate cation arrangements is evident in the crystal-structure differences of silica and lithium disilicate. The composition intermediate

between silica and lithium disilicate corresponds to $Li_2O \cdot 5SiO_2$ and if it is attainable by crystalline solution at all, a possible reconstruction that might enhance the process is inversion on each side of an appropriate diffusion couple to a crystalline solution of Li_2O in SiO_2. Materials that appear to be single-phase crystalline solutions have been prepared in the composition range between $Li_2O \cdot 2SiO_2$ and $Li_2O \cdot 3SiO_2$.

Much of the foregoing is conjecture. Nevertheless, it is apparent that crystalline solutions should not be expected to have phase homogeneity over any extensive composition range. Crystalline solution by displacement of Li^+ ions with Si^{4+} ions seems to be possible at compositions between about 25 and 33 mol percent lithia, and crystalline solution of Li_2O molecules into tridymite and cristobalite seems to occur at zero to five mol percent lithia compositions, but otherwise, crystalline solutions may not even exist.

Vitreous combinations are different. The glasses are amorphous mixes of minute molecular clusters with short-range order. They might even be considered as degenerate crystalline substances that are so defective that the only recognizable crystallinity remaining is on a short-range basis. The same "order" or "crystallinity" need not be displayed by separate molecular clusters. In any case, there are many channels for diffusion, and many vacancies are available for occupancy by a wide variety of species. The main difficulty in

trying to form silica-lithium disilicate glasses is that because of the very lack of extensive order that permits interpenetration, they are inherently unstable or at best metastable. They can achieve greater stability by crystallizing, but to do this they apparently need compositions near the regions of crystalline solution. Thus, if net compositions between about 5 and 25 mole percent lithia are involved, a tendency toward phase separation is suspected as a first stage of devitrification. This is one argument that leads to a prediction of a liquid miscibility gap in the silica-lithium disilicate sub-system. The belief also has been fostered by thermodynamic calculations, measurements of electrical conductivity, inferences from the behavior of other silica systems, by devitrification behavior, and conversely by thermal clearing of an opalescence that can be annealed into the glasses. The behavior mentioned last has been the basis of the only previously reported measurements of the liquid miscibility boundary (1, 26). These measurements are displayed together with a thermodynamically calculated boundary (8) in Figure 2. The corresponding phase separation is generally presumed to occur by a spinodal mechanism. Implications from a later section of this report have been added as data points in the figure, for comparison. The data of reference (26) are qualified because they were based on electron micrography of separated phases, presumed to be essentially binary, in ternary Li_2O-Na_2O-SiO_2 and Li_2O-K_2O-SiO_2 systems. The

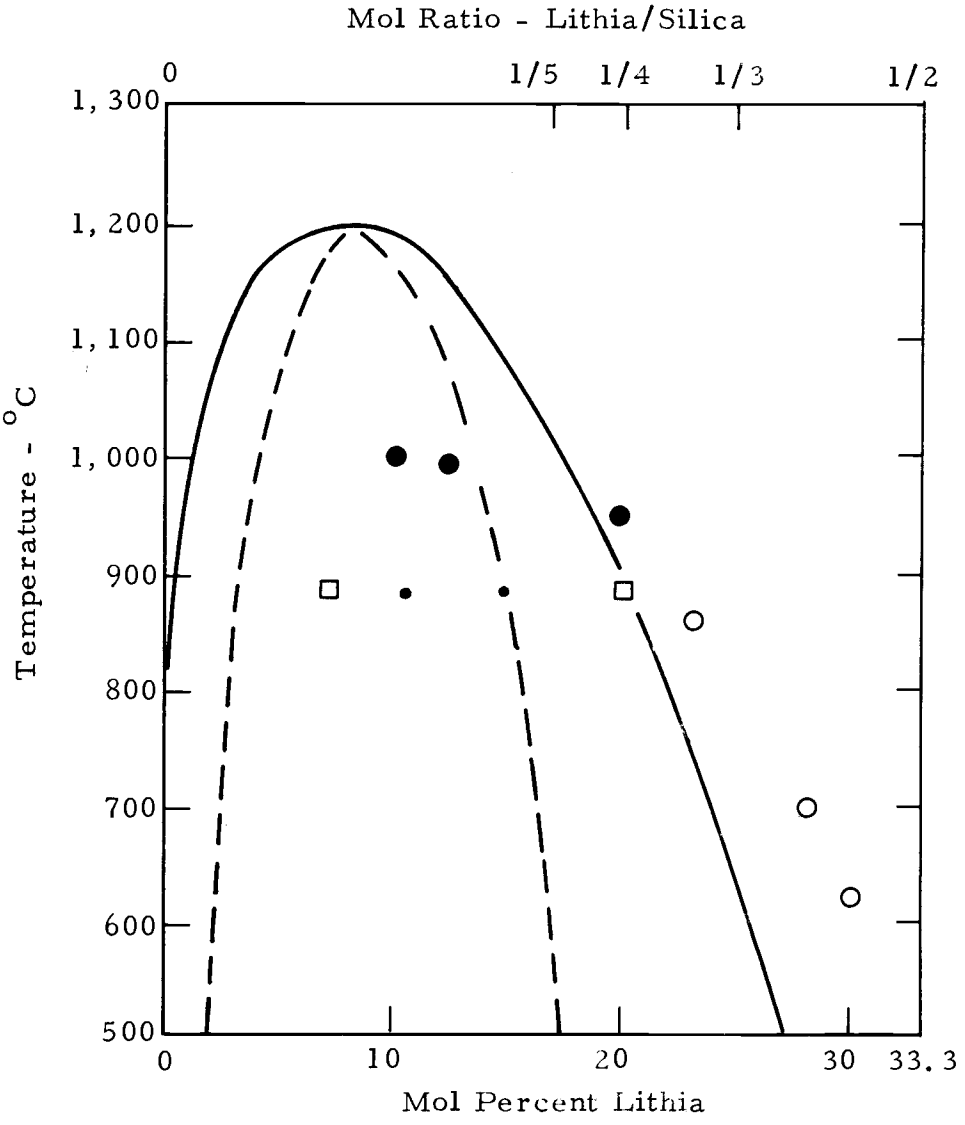

Figure 2. Liquid immiscibility between silica and lithium disilicate. (curves - ref. 8; ● - ref. 26; ○ - ref. 1; □ , • - this work; broken line and small dots are spinodal estimates)

miscibility boundary should be viewed in conjunction with Figure 1.

Clear vitreous glasses may be prepared, without unusual difficulty, with net compositions between about 20 and 33 mol percent lithia, or roughly from $Li_2O \cdot 4SiO_2$ to $Li_2O \cdot 2SiO_2$. But at compositions richer in silica, melting temperatures become high enough to tax the heating equipment and crucible materials that are usually available. Those silica-rich specimens that have been prepared despite difficulties have been characterized by a bluish opalescence, sometimes by severe cracking, and occasionally by spontaneous devitrification. The devitrification behavior of the glasses containing 20 to 33 mol percent lithia is barely distinguishable from that of pure lithium disilicate. This is another observation that may imply a liquid-liquid separation before devitrification, so that it is a phase with a composition near lithium disilicate that actually undergoes the devitrification.

EXPERIMENTATION

Preparation and Diffusion of Specimens

The general plan of experimentation was to combine pure silica with various silica-lithium disilicate glasses by diffusion, then to use neutron-induced autoradiography to study the distribution of lithium in the gradient of compositions formed, and finally to evaluate the lithium distribution for evidence germane to immiscible behavior. New information was sought concerning both the application of neutron-induced autoradiography and the nature of silica-lithium disilicate compositions.

Materials

Fortuitously, glasses in the desired composition range had been prepared as a part of a previously completed investigation (19, 27) and they were available for reuse. The specimens are identified in Table 2. The lithia contents were determined by flame photometry, but the silica contents were determined by a wet chemical analysis. The photometric method is considered more accurate. Analyses for impurities, including Al, Cu, Fe, Mg, Na, and Ti, indicated total contamination was less than 0.5 weight percent in each case. The specimens were in the form of short cylinders, 5/16 inch or 1/2 inch

in diameter, that had been vacuum induction melted in a graphite crucible.

Table 2. Lithia-Silica Glass Specimens

Code Symbol	Weight Percent		Mol Percent		
	SiO_2	Li_2O	SiO_2	Li_2O	$Li_2O \cdot 2SiO_2$
H3	77.9	20.2	63.8	33.6	~100
H4	80.5	19.0	67.4	31.9	95.7
H5	81.5	17.2	68.8	29.3	87.9
H6	87.3	11.8	77.5	21.1	63.3

For use in conjunction with the lithia-silica glasses, some 5/16-inch-, and 1/2-inch-diameter rods of quartz glass were purchased. This is an optically clear, vitreous material that the manufacturer specified to be 99.97 percent pure. The principal impurity is alumina.

Equipment

Three major units of equipment were used: a vacuum hot-press, a small electron-bombardment heating furnace of ten kilowatts power capacity, and a tube furnace rigged for a flow of argon through the tube. These were augmented by a typical assortment of cutting, grinding, and polishing machines, and some optical microscopes for examination of surfaces.

The vacuum hot-press apparatus is enclosed in a vacuum chamber with walls of water-cooled copper. The chamber is cylindrical, about 15 inches in diameter. For this work, the chamber was pre-evacuated to pressures of about 10^{-3} torr or slightly less using a compound rotary-piston pump. Operating pressures were 10 to 100 times higher. Heating is accomplished by a flow of direct current through a tubular graphite resistor, coaxial with the chamber. The heater is nominally three inches in diameter. Graphite parts are of a dense grade with good purity and homogeneity (National ATJ, AUC, AGMT, or equal). Inside the hollow heater is another tube of graphite into which simple graphite dies and punches of various sizes are fitted within the limitation of a 1.5-inch maximum diameter. The die and the lower punch are statically mounted, but the upper punch may be dynamically loaded. The loading is done either by transmitting force from a 750-pound hydraulic load cell through a stainless steel bellows, or by simply allowing the differential pressure of the external atmosphere to operate on the effective area of the bellows end-plate. There is a longitudinal slot in the heater, so that an optical, disappearing-filament pyrometer may be used to measure temperature on the outside surface of the inner tube that contains the die and punches. When, after a period of adjustment, the temperature reaches a steady value, it is taken as the equilibrium temperature of the entire punch and die assembly. Pyrometer sighting is done

through a small Pyrex window with a magnetically operated shutter.

The heating by electron bombardment was also done in a vacuum chamber, basically of water-cooled copper construction but with an inside diameter of about seven inches. Evacuation in this case was by means of a 500-liter-per-second oil diffusion pump working in tandem with a seven-liter-per-second rotary-piston compound pump through a water-cooled trap. Pressures as low as about 10^{-6} torr are attainable, but operating pressures are usually at least an order of magnitude higher. Inside the chamber is a work-accelerated electron-bombardment system. Electrons are emitted from four thermionic filaments of 30-mil thoriated tungsten wire, arranged radially, 90° apart, in a horizontal plane above a stool or pedestal of water-cooled copper. The emitters are resistively heated by an alternating current. The filament assembly and the stool are symmetrically aligned on a common vertical axis. The spacing between them is variable. An object or substance to be heated is placed atop the stool and bombarding electrons are accelerated to it by applying a direct-current potential between the filaments and the stool. Potentials up to about 12 kV can be applied in this equipment, and currents are normally limited to about one ampere. The electrons are not focused except by a convergence of the field lines because of inherent geometry. The system is operated with a positive ground connection. Heating can be observed through a double-paned window -- Pyrex on

the inside, Plexiglass on the outside.

The "tube" in the tube furnace is alumina, it has a bore of about 1.5-inch diameter, and it is 12 inches long. It is wound with a resistance heater of Smith "Tenalloy", rated for temperatures to 1,200°C. Primary power for heating is drawn from a 110-volt a c line, stepped down with a continuously variable autotransformer. Temperature control is maintained by a potentiometric on-off controller (Brown "Electronik") calibrated for a chromel-alumel thermocouple sensor. The control thermocouple is imbedded in insulation immediately outside the alumina tube and its heating coil. The controller has built-in electronic temperature compensation. Argon is tapped from a steel cylinder through a constant-pressure regulator and flow gage at 15 psi. It is piped to the furnace through Teflon tubing, and is bled into the rear of the furnace tube through a short length of silica tube. Wads of silica wool are used as permeable plugs in both of the tube openings. The temperature inside the tube is measured with a Pt-Pt/10%Rh thermocouple connected to a multi-range potentiometric recorder (Varian G-14). This recorder is not temperature compensated, so the circuit includes a reference junction at the recorder terminals. Ambient temperature is read frequently from a mercury thermometer and the thermocouple output must be corrected by a corresponding amount. Temperature profiles, excluding two inches at each end of the tube, were measured at approximately

500° C, 900° C, and 1,100° C. In addition, the correspondence between controller settings and actual temperatures was checked at seven temperatures. It was discovered that to the rear of a point about 5.5 inches into the tube, the temperature profile could be considered completely flat within the control fluctuations. Temperature gradually decreases toward the front, reaching a minimum at the tube mouth about 100° C below the maximum toward the rear. Calibration of the rear temperature in terms of the controller setting is shown in Figure 3. The dependence is slightly nonlinear. The bars shown indicate the range of cyclic fluctuation at each setting.

Procedures

The first attempts at diffusion couple preparation were made in the vacuum hot-press. Cylinders, about 1/2 inch long and 5/16 inch in diameter, of the H3 composition and the clear quartz glass were prepared by lapping one end flat using a series of abrasives down to three-micron diamond. The cylinders were loaded in a hot-press die with the flattened ends in contact with each other. Loading on the punch was limited to that due to the vacuum -- probably in the order of 1,000 psi on the 5/16-inch punch. To help allow for non-flattness and non-squareness, discs of graphite foil were inserted between the punch ends and the specimens. In three attempts at joining the cylinders, at temperatures between 900° C and 1,000° C

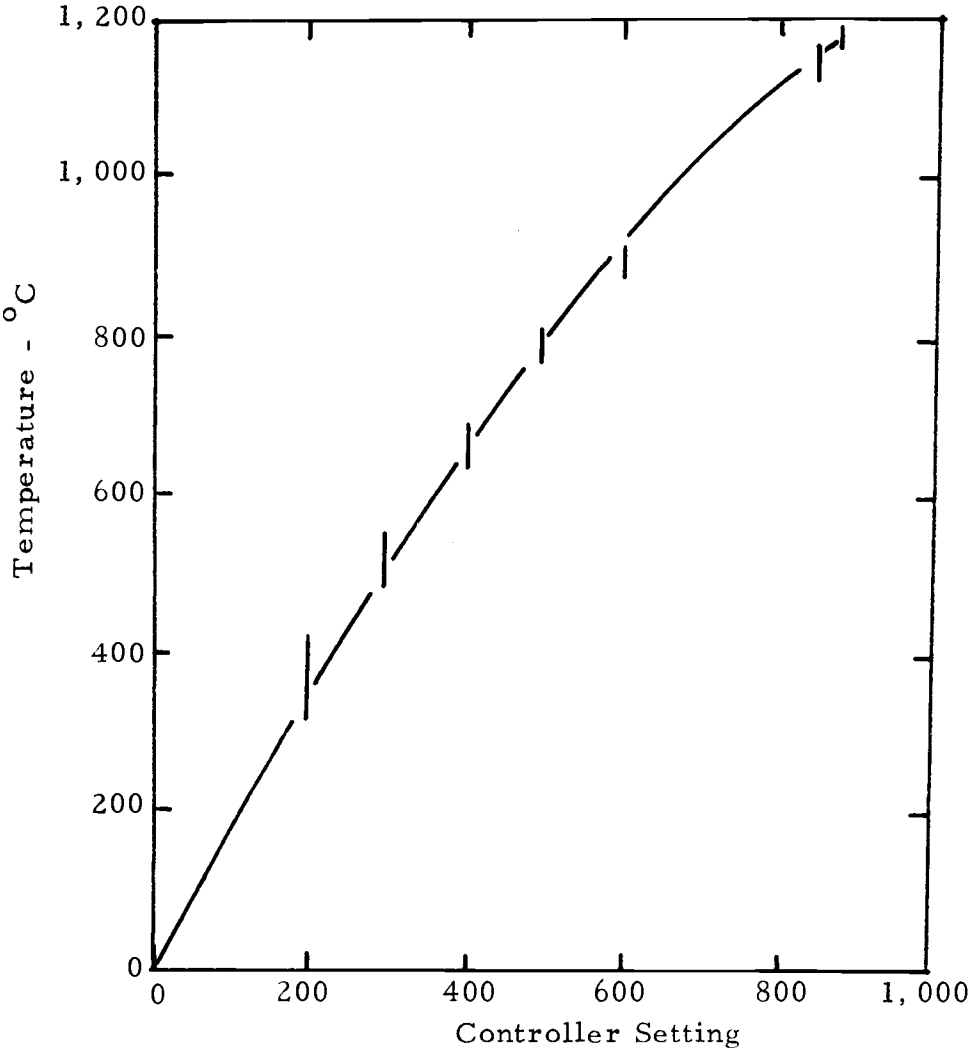

Figure 3. Tube furnace calibration.

for times up to four hours, there was no evidence of an interaction.

The electron-bombardment furnace was used in all other couple preparation work. First, some more solid-state joins were attempted using the spring-loaded arrangement sketched in cross section in Figure 4A. The couple materials were placed in a diametric hole in a graphite cylinder. They were pushed together by spring pressure transmitted by two graphite plungers. The entire graphite block was heated by electron bombardment. The temperature was monitored by sighting an optical pyrometer through the double window from a point behind a magnetically operated shutter into a small hole drilled into the front of the main graphite block to intersect with the couple well at a point where the couple materials should meet -- that is, by sighting on the interface to be joined. The solid-state joins were no more successful here than they were in the hot-press furnace. However, on a pair of occasions, the temperature was raised too high, the H3 material melted and was extruded out through the pyrometer sight hole and back along the loose-fitting spring-loaded plungers. When this happened, there was also some sign of reaction between the H3 material and the silica. So it was decided to try to contain the H3 material as it was melted against the silica. A niobium sleeve was inserted in the couple well. This sealed off the pyrometer sighting hole and provided for tighter-fitting plungers. The molten H3 was successfully contained, but there was a severe reaction with the

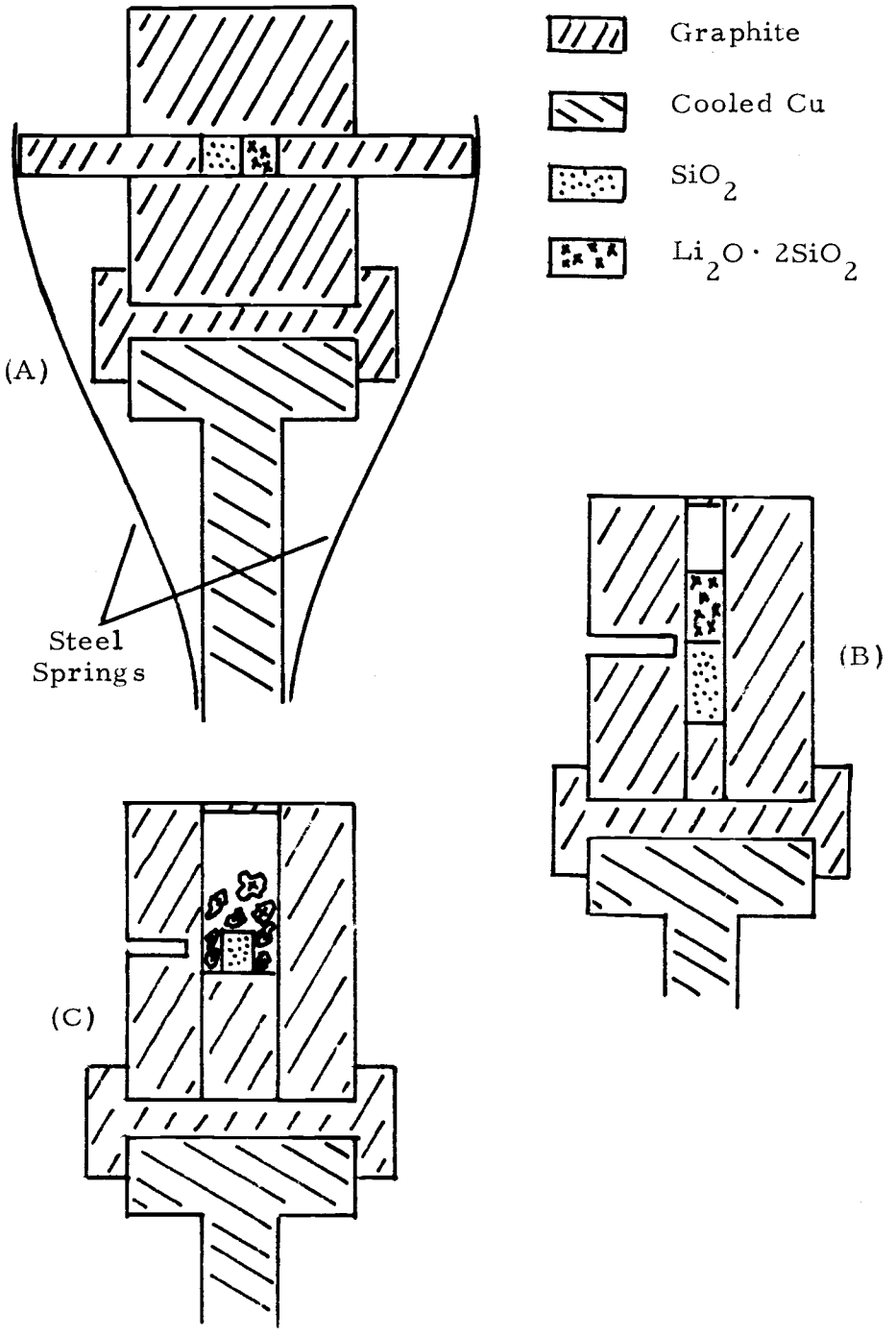

Figure 4. Specimen preparation schemes, electron bombardment heating.

niobium.

The next scheme tried is sketched in Figure 4B. At the left of the sketch is a pyrometer sighting hole, which was oriented toward the front of the furnace. The couple well in this case was vertically oriented, and the plan was simply to melt the H3 on top of the silica. There was consistent evidence of reaction between the two materials. But apparently because of shear stresses due to differential shrinkage, the interface was just as consistently fractured by the time the couple was removed from the well. This experience led to the final approach used.

Figure 4C illustrates the procedure that has been most successful in preparing couples. The vertical couple well was enlarged to a 1/2-inch diameter. A 5/16-inch-diameter cylinder of clear silica is centered at the bottom of the well, and enough H3, or one of the other silica-lithium disilicate compositions, is charged to completely cover the silica when the lithium-bearing glass is melted. About 0.75 gram of silica and 2.0 to 2.5 grams of H3 are typically involved. It seems that unless the silica-lithium disilicate glass has been previously "fined" in vacuum, it should be held molten for at least an hour before quenching, in order to avoid devitrification during solidification.

The graphite used in the electron-bombardment furnace was of high quality similar to that used in the vacuum hot-press. Although

the environment was thermodynamically favorable for a reaction between silica and carbon (18), no evidence of an interaction was detected. Perhaps the lithium-containing glasses that were in contact with the graphite are more inert with respect to carbon, or perhaps surface tension prevented a sufficiently intimate contact.

At one time, an effort was made to control more closely the temperature during diffusion couple preparation by using a W-W/26%Re thermocouple in the electron-bombardment furnace. But the electric fields associated with the heating interacted with the thermocouple so erratically and uncontrollably that the output was meaningless. Another improvement was more successful. This was a modification to blow helium gas against the heated graphite to accelerate cooling after the heating power is shut off.

Four useful couples were prepared with the H3 composition combined with silica. One other was prepared with H5 material combined with silica. For identification, they were assigned numbers corresponding to the dates of their preparation: 121867, 122867, 011168, 021268, and 031169. The last one listed is the one involving the H5 glass, and it was prepared too recently to be used in further experimentation yet. One couple, 011168, was contaminated by both boron and platinum during preliminary diffusion trials. As a result of the experience, boron nitride and platinum were each rejected for use as diffusion boats. Instead, alumina boats are used, but

contact between the couples and alumina is avoided by nesting the couples in a bed of silica wool in the boat. In this way, three uncontaminated couples were annealed for 186.4 hours at 896 $\pm$ 14° C. Then couples 122867 and 021268 were annealed for 163.9 hours more at 878 $\pm$ 22° C. Of these, couple 122867 has been a subject of autoradiographic study.

The couples are illustrated in Figures 5 through 8. Figure 5 is a general view of couple 031169. Although the lithia-bearing glass on the outside cracks as it contracts against the silica inside, the couples are quite durable in normal handling. Except for the cracks, the outside parts of the "good" couples were, however, clear vitreous materials. Figure 6 shows the joint between the inner and outer parts of couple 031169 in as-cast condition. This is part of the surface on which the couple is resting in Figure 5. Figure 7 is a view similar to that in Figure 6, except that the surface has been polished here. It is apparent that despite the cracking, there are fairly large regions of reasonably good contact between the couple materials. Figure 8 shows the joint region of couple 122867 after both diffusion and autoradiography. The H3 disilicate on the outside is devitrified, the silica is not, and between them is a band of opalescent material. Some healing of smaller cracks is evident also. It is quite possible that if a central silica cylinder of smaller diameter had been used, much of the cracking problem would have been avoided.

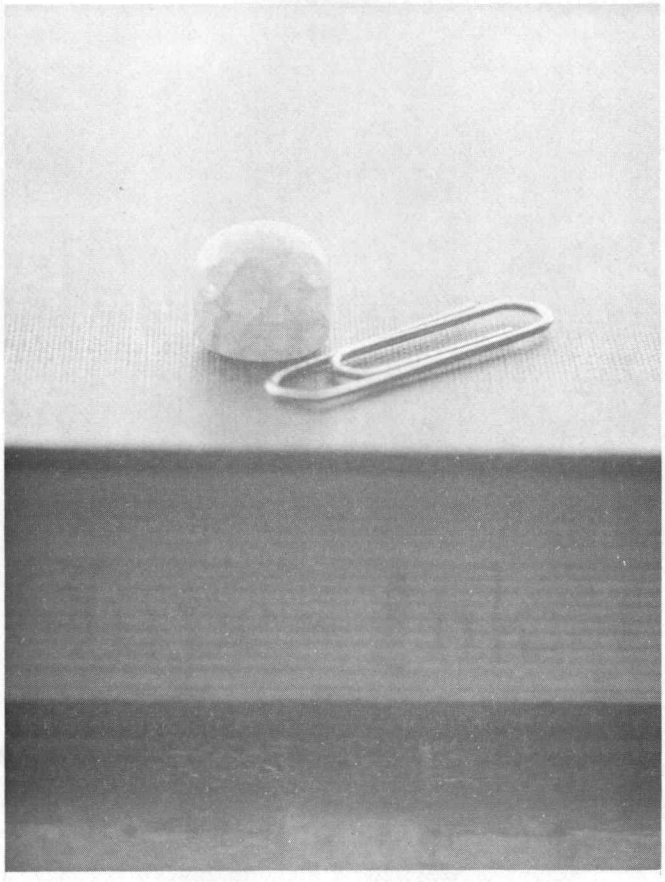

Figure 5. Diffusion couple 031169.

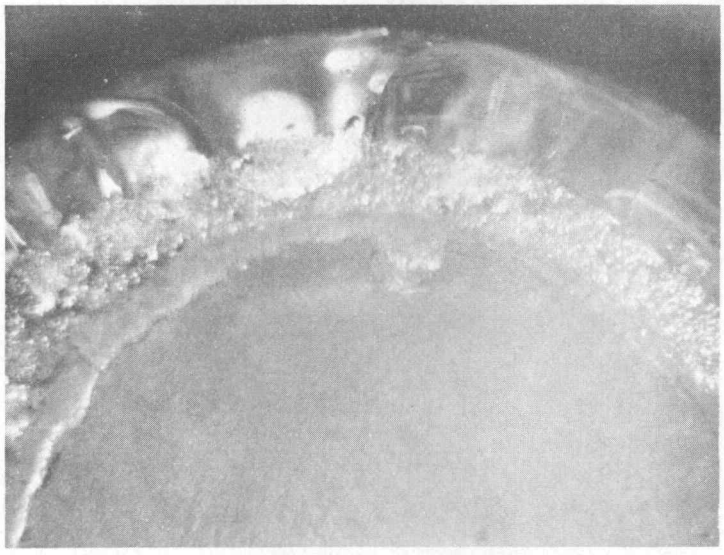

Figure 6. Joint between glasses, couple 031169, as cast, 12X magnification.

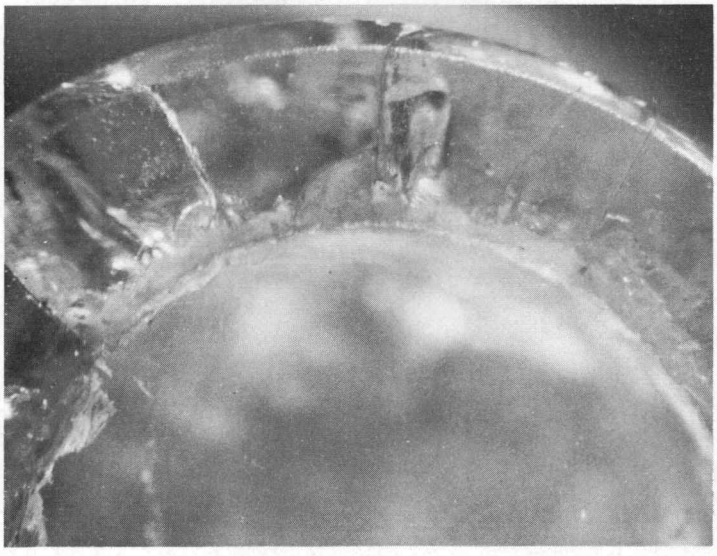

Figure 7. Joint between glasses, couple 031169, after polishing, 12X magnification.

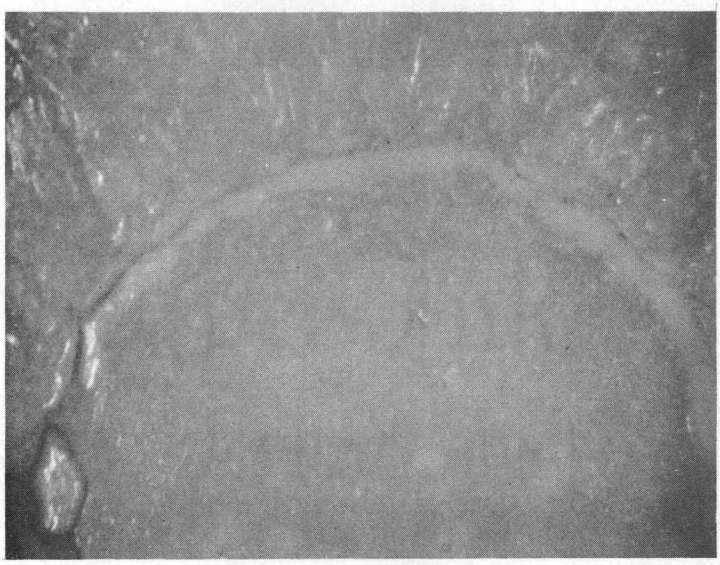

Figure 8. Joint between materials, couple 122867, after diffusion and autoradiography, 12X magnification.

Preliminary Autoradiography

Fundamentals

The distribution of lithium at the surface of solids such as those involved in this work may be detected by means of alpha-particle ejection by captured thermal neutrons according to the reaction $^{6}Li(n,\alpha)^{3}H$. The neutron-capture cross section is about 910 barns. The natural abundance of ^{6}Li is 7.52 percent, and the isotope is one of a relatively few light-element isotopes that undergo a neutron-alpha interaction with slow neutrons. Lithium is not activated by thermal neutrons to a radioactive state that decays over any appreciable half life. Because of their bulk and double charge, the liberated alpha particles interact strongly with matter and have a short range. Thus, only those originating within a few molecular layers of a surface can emerge, and these are capable of only shallow penetration into another solid in contact with the source material. The dissipation of energy in the stopping medium results in damage, and if the damaged substance is composed of large, weakly-bound molecules, the effects of the damage are especially extensive. At best, however, the damage tracks are not apparent by normal examination unless the tracks are somehow enlarged. A common way of doing this is to use the preferential tendency of an etchant to attack strained, damaged, or other energetic sites. Polymers are

materials with suitably large, weakly-bound molecules, and among convenient polymers, nitrocellulose plastic is relatively unstable and therefore sensitive to both alpha damage and etchant attack. It was selected for use as the dielectric detector in this work. The suitability of cellulose nitrate and sodium hydroxide as a detector-etchant pair for use with alpha particles has been demonstrated previously (11).

The basic procedure adopted for autoradiography is to prepare a specimen surface by grinding and polishing, then place it in firm contact with a piece of cellulose nitrate sheet while both the specimen and detector are irradiated with thermal neutrons in the Oregon State University TRIGA-III research reactor. The appropriate irradiation levels are in the orders of 10^9 to 10^{10} neutrons/sq cm. Later, the plastic film is developed by etching in a 6N solution of sodium hydroxide. Thus, the damage tracks are rendered visible at reasonable magnifications. Their density and distribution are related to the concentration and distribution of lithium at the surface of the specimen. Both the neutron-alpha reaction and the damage-tracking process are statistical in nature, and they are subject to normal fluctuations even under ideal conditions. In addition, errors, biases, or uncertainties can be caused mainly by a non-uniform or uncertain neutron flux during irradiation, by a non-uniform or inconsistent response of the plastic film to either alpha penetration or etching,

and by a dependence of track density measurements on human judgement. Many irregularities of plastics behavior have been discussed in a comprehensive dissertation, recently published (3), and they are far beyond the scope of this discussion.

The specimens for autoradiography have already been described. Two sources of cellulose nitrate sheet were used. In the earliest experiments, film was obtained by cutting sections from plastic vials stocked for use in Beckman chromatographic apparatus. Nothing is known of this material except that it is basically nitrocellulose and that its optical properties, at least, must be controlled in order to assure reproducible chromatography. Because the vials were cylindrically curved, the sections had to be flattened by annealing at about 100° C for 30 to 60 minutes while the plastic was clamped flat between microscope slide glasses. Later, some 35-mil rolled sheet was purchased from the Standard Pyroxoloid Corporation, Leominster, Massachusetts. This company's product normally contains about 25 percent by weight of synthetic camphor as a solvent plasticiser and traces up to a few percent of an alcohol secondary solvent, in addition to nitrocellulose. The alcohol gradually evaporates during the first two or three months after the plastic is manufactured. The camphor too has a fairly high volatility, so definite aging behavior might be expected from the plastic. The exact date of manufacture is not known, but the shipping date was February 7,

1968, and all irradiations reported here were completed by July 5, 1968. It is significant that latent tracks were stored in the plastic for times up to four weeks before development.

Neutron irradiations were accomplished in the "lazy susan" irradiation rack of the TRIGA-III reactor. Specimens to be irradiated in this mechanism are enclosed in "TRIGA-tube" specimen holders especially designed for the function. The stock TRIGA-tubes are made entirely of clear acrylic thermoplastic, and these were used in the first irradiations. The nitrocellulose films were prepared as 3/4-inch discs and placed at the bottoms of approximately cylindrical (actually slightly tapered) cavities in the TRIGA-tubes. Lithia-silica specimens were centered on top of the films and wedged there by stuffing the rest of the tube cavity with soft, elastic rubber. Later, the effect of the acrylic plastic in distorting the neutron flux was questioned, and to avoid the possibility, some special TRIGA-tubes were machined from aluminum. These retained the outside dimensions necessary to fit the lazy-susan receptacles, but internally they were more specifically designed for the particular specimens involved in this work. The specimens are constrained and centrally positioned in these holders by aluminum rings of various sizes to match the various specimen sizes used. Each specimen is also pressed against nitrocellulose film by an internally mounted coil-spring of zirconium. The holders are loaded and unloaded, and parts

assembled and disassembled by means of two threaded joints.

Alpha damage tracks in irradiated films were developed by etching in a laboratory beaker, using 6N NaOH solution. Films were held upright and well-separated by wedging them edgewise into shallow slots cut in a piece of Teflon plastic. No agitation or stirring of the etchant was employed, and it was assumed that room temperature would be stable enough to avoid problems of temperature control and reproduction. Etchant solutions were always mixed far enough in advance to be sure that they were at ambient temperature when they were used however. In general, the reuse of etchant was avoided to obviate depletion of strength, and accumulation of impurities. In retrospect, more careful temperature control may have been in order. Developed films were examined microscopically, usually at 100X or 400X nominal magnifications. A calibration revealed that the higher magnification was actually 428X.

Calibration

The first goal of autoradiography was to calibrate the method as a function of lithium content. Five experiments have been completed. Each experiment involved the four "standard" compositions, H3, H4, H5, and H6. The notation used to keep track of experiments was to add a parenthetical number suffix to the specimen number to identify the irradiation. Thus, H3(1) designates the first irradiation

of specimen H3.

Data in Figure 9 resulted from the first and second irradiations, corresponding to 10 kw-sec and 40 kw-sec of nominal reactor energy respectively. The microscope used to examine developed film has a provision for projecting the magnified image onto a ground glass screen or onto a Polaroid film. In experiments one and two, the ground glass was used. A window of four sq cm was masked off on the screen, and numbers of tracks in this area were counted directly, then corrected for the magnification factor. Each point in the figure is an average of five determinations, and the bars indicate the scatter of individual determinations. Acrylic TRIGA-tubes and the Beckman plastic film were used. The linearity of track density with lithium content is reasonable, but the track density also should be proportional to the reactor energy, which determines the total number of impinging neutrons. This behavior was not indicated. Later, it was realized that the apparent lack of linearity with reactor energy was really a problem of correct track counting. Irradiation energies of 25 and 40 kw-sec are simply too high in the sense that the resulting track patterns are so dense that there is excessive superposition of tracks, and the track counts are invariably too low. An autoradiograph typical of such circumstances is shown in Figure 10.

Another problem encountered early but not really recognized until later concerned inconsistencies in etching plastics. Tracks

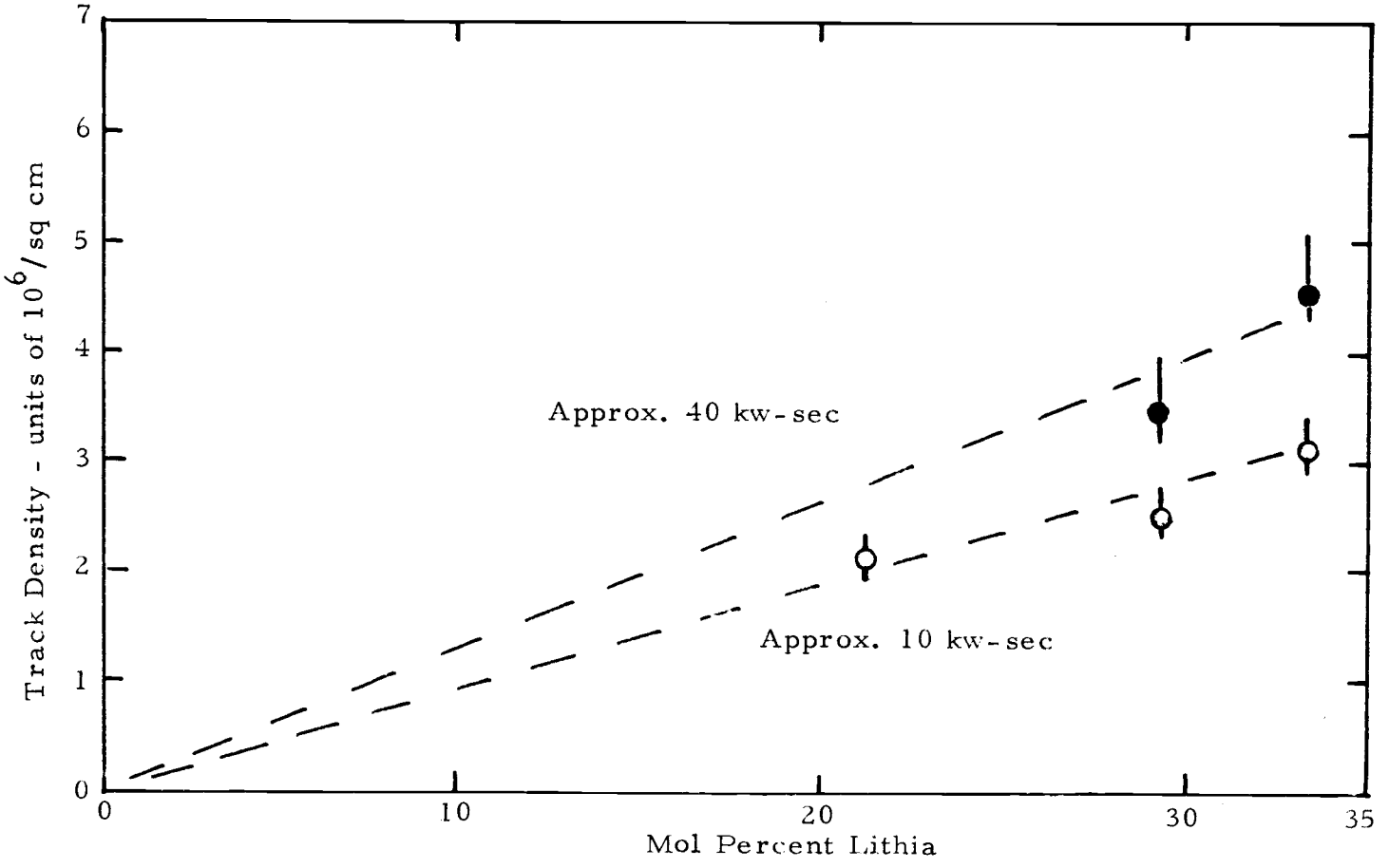

Figure 9. Calibration experiments one and two.

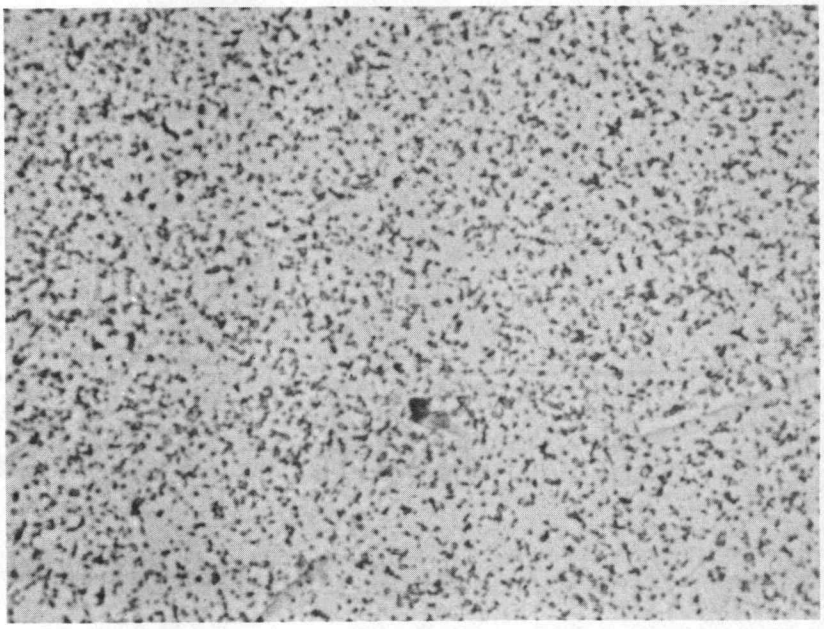

Figure 10. Etched alpha tracks in cellulose nitrate, resulting from 25 kw-sec irradiation of specimen H3 by thermal neutrons, with an apparent track density of about 6×10^6 per sq cm, magnified 400X.

were well defined in H3(1), H6(1), H3(2), and H5(2) after 30 minutes of development, but 45 minutes were required for H5(1), and even after an hour of development, no tracks could be seen in H4(1), H4(2), and H6(2). As long as care is taken to insure that new track pits are no longer being developed in each autoradiograph, the correctness of track counts does not seem to be affected by variations of etching times. However, overetching is undesirable because it enlarges the pits making it more difficult to resolve them from each other, and making it more difficult to distinguish actual tracks from minor flaws in the plastic detector. In addition, the lack of a standard procedure because of etching time differences necessitates incremental etching and much extra examination of autoradiographs to check on etching progress. It is in regard to this problem that better control of etching temperature might help.

In experiment three, which resulted in Figure 11, the Standard Pyroxoloid plastic was used, but the acrylic TRIGA-tubes were still in service. The nominal energy was 25 kw-sec. Magnified track images were photographed in this case, and counting was done in four-sq-cm areas on the photo prints. Nitrocellulose films were first developed for one hour. Six track-density counts were made for each specimen, and averages with scatter bars are plotted in Figure 11. The result was not very satisfying, so the films were etched an additional 30 minutes. This time three determinations were made for

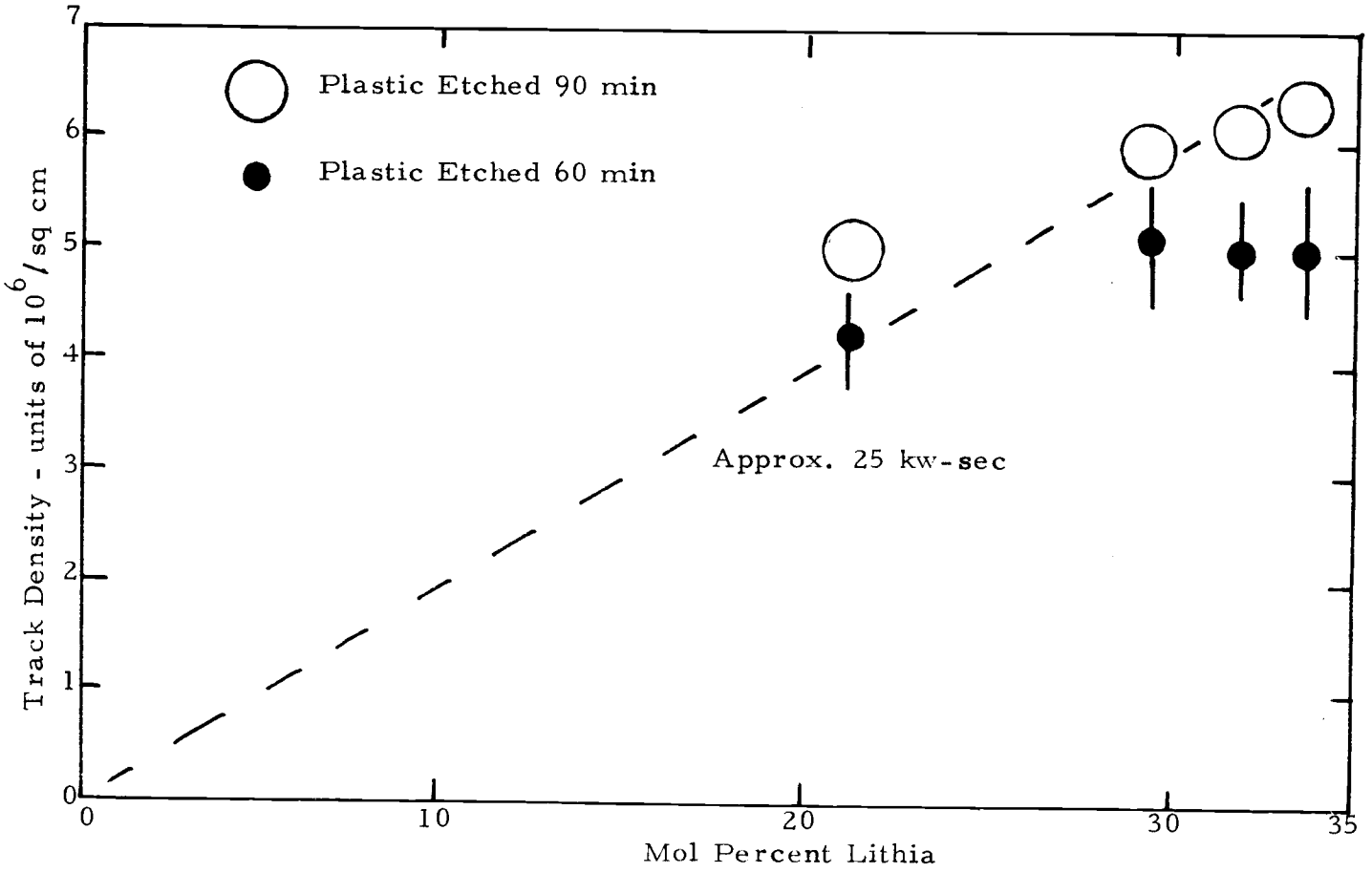

Figure 11. Calibration experiment three.

each specimen, and the corresponding circles in Figure 11 are drawn large enough to encompass all three. The experiment amplified questions about proper etching times and excessive irradiation energies.

At about this time, a third problem became apparent. Throughout these experiments, the nominal power at which the reactor was operated was multiplied by the measured irradiation time to obtain approximate irradiation energies. Evidently this is not a very accurate method of estimation. For good quantitative accuracy and reproducibility, it would be necessary to devise a means of monitoring the actual irradiation exposure of the autoradiographic specimens. Rather than divert effort in solving this problem, the expedient alternative of accepting relative calibrations was adopted for the time being. That is, in the remaining experiments, each calibration was done in conjunction with an irradiation of a diffusion couple. Thus each attempt to determine unknown compositions was based on a separate and specifically related calibration. However, it turned out that the separate calibrations at lower reactor power were not markedly different from each other.

Overall, of the problems encountered in autoradiography, one of the more serious things, and certainly the most annoying, was the tedious pit-by-pit procedure of counting tracks. The situation will require considerable improvement if this sort of autoradiography

is to be extensively applied. Perhaps there are relevant measuring techniques to be learned or borrowed from the instrumentation of secondary-electron microscopy and microprobe x-ray microscopy, where somewhat similar images must be viewed.

Experiments four and five comprised irradiations of both standard specimens and diffusion couple 122867. The aluminum TRIGA-tubes were available for use as well as the newer supply of plastic film. Both experiments were nominally at a three-kw-sec energy level. Track pits were counted by overlaying photographic prints with a piece of window glass and using a marking pen to keep track, on the glass only, of which pits were counted. The main differences between the experiments were that in the fourth the plastic film was annealed for an hour at 100° C before irradiation, and in the fifth the film was exposed to ultraviolet light at 30 inches from a fluorescent lamp for an hour after irradiation but before etching. Neither experiment included both of these procedural variations. Calibration results as shown in Figures 12, 13 and 14 also reflect some variations of etch times and counting practice. The etching times were 120 minutes, 150 minutes and 60 minutes, respectively. For Figure 12, two complete sets of photographs were taken, and the total area (91.6 sq cm) of each frame was counted. In Figures 13 and 14, the whole-frame technique was compared with separate counting of five sections of each photo frame and adding the section counts

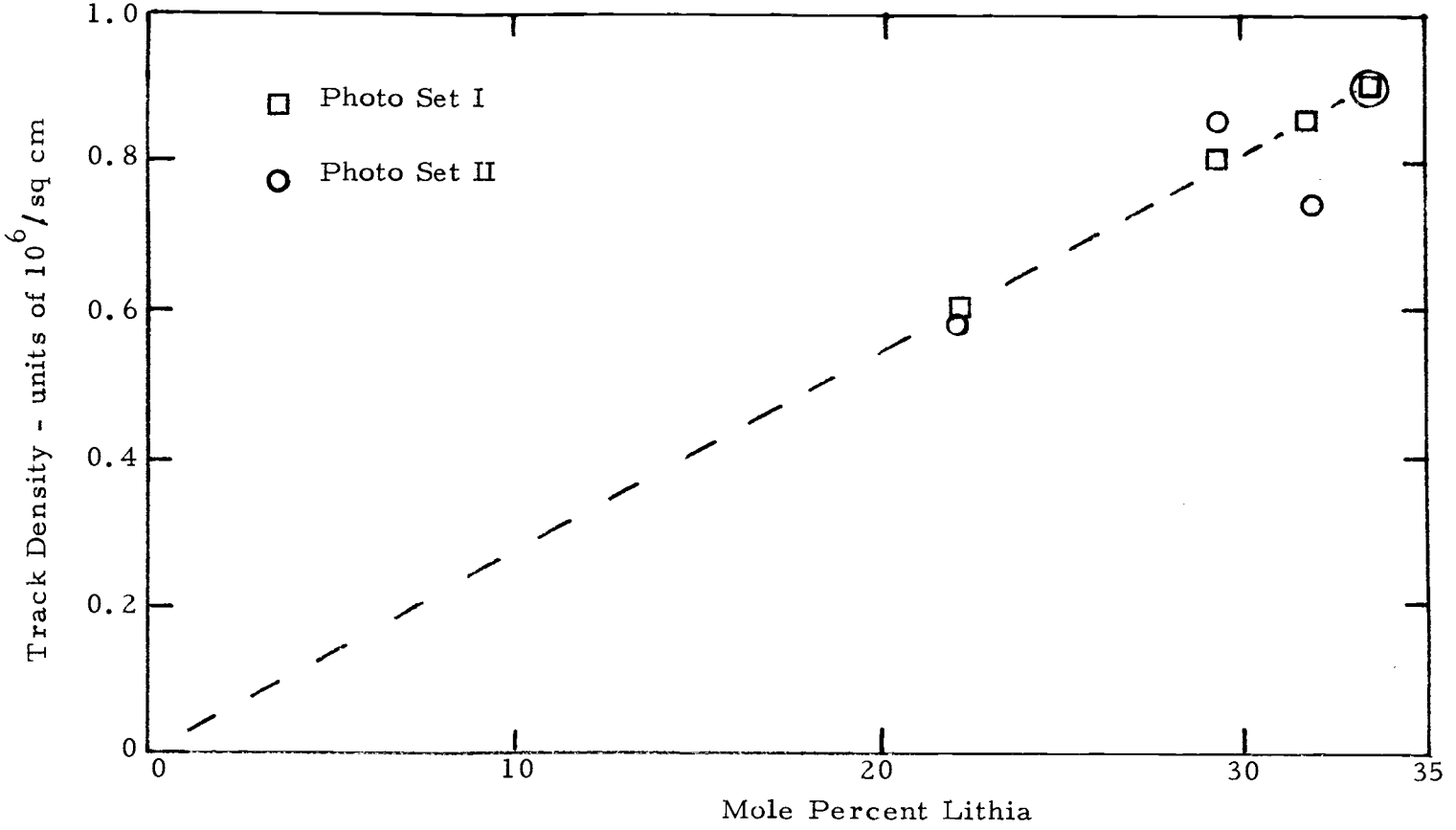

Figure 12. Calibration experiment four-A.

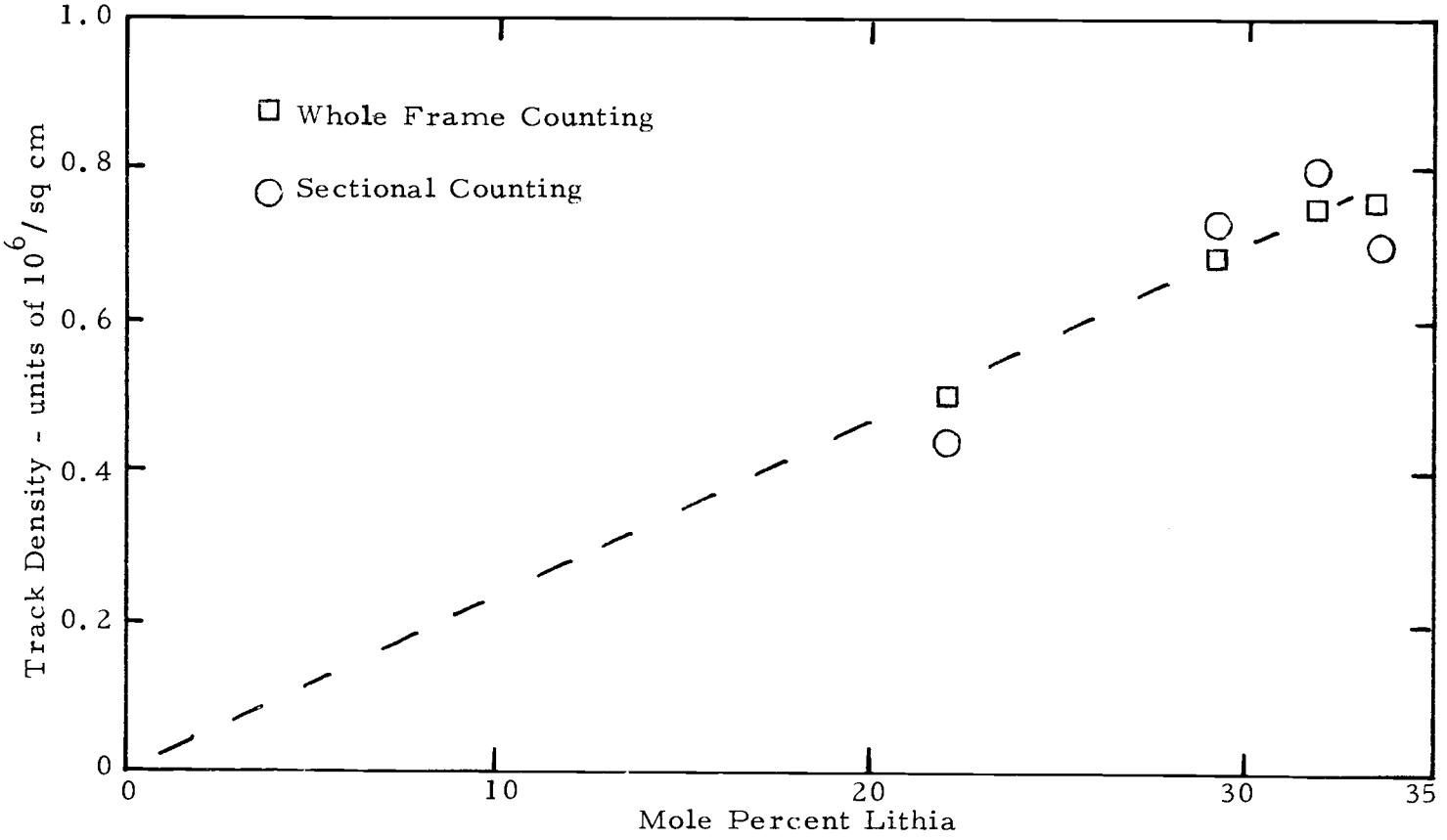

Figure 13. Calibration experiment four-B.

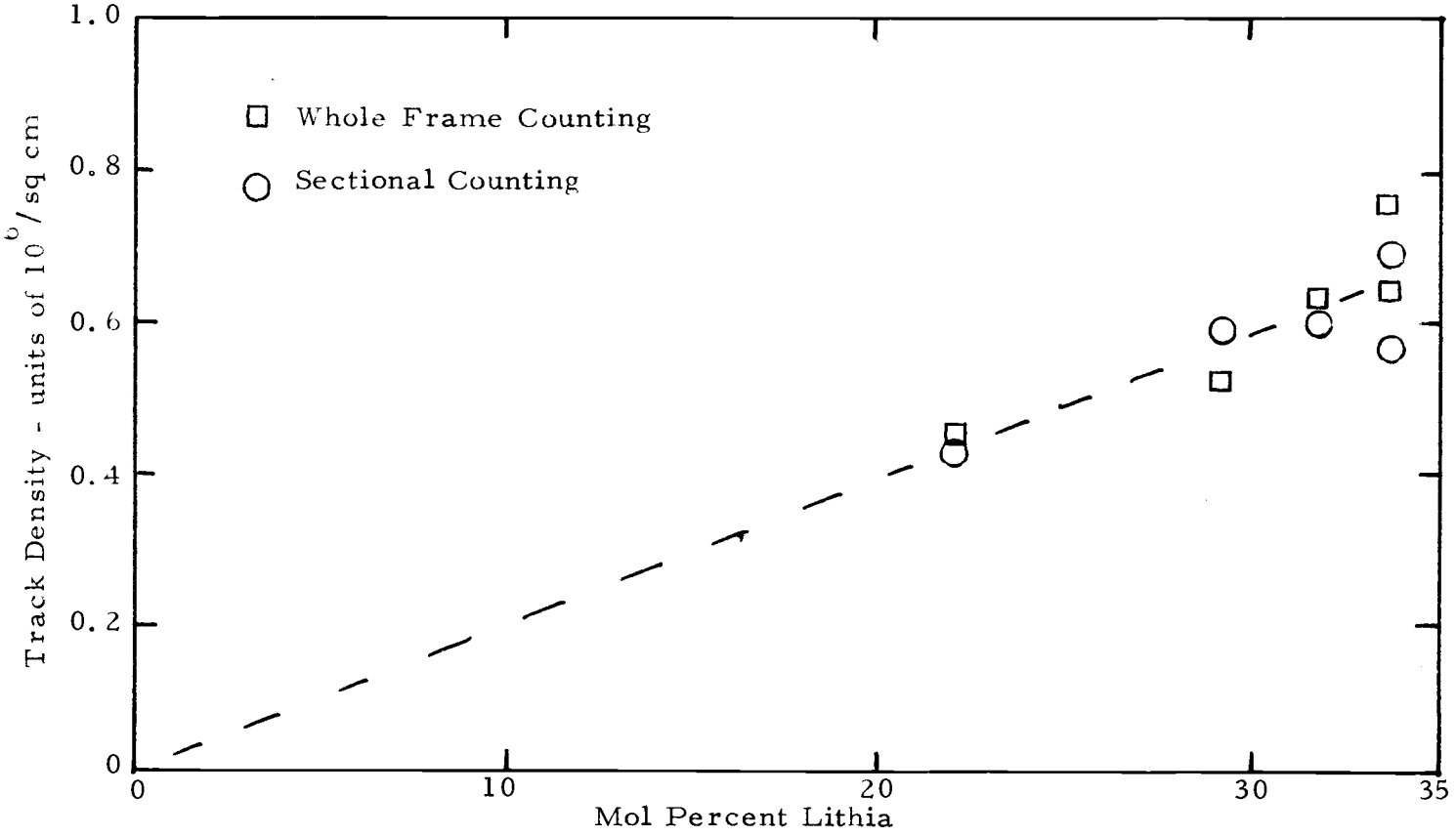

Figure 14. Calibration experiment five.

together. The effects of prior annealing and post exposure of plastic film to ultraviolet light were not pronounced, although the ultraviolet may have decreased the required etch time. Overall, the results of experiments four and five were an improvement over earlier results. Although a further reduction of scatter is needed, the experiments agreed fairly well with each other.

A composite calibration at three kw-sec, from the combined results of experiments four and five, is presented in Figure 15. For comparison, the results of experiment one at ten kw-sec are also repeated. The gradients are steep enough to indicate a reasonable inherent sensitivity to compositional differences. Considering that the irradiation energies are only approximate, the expected proportionality between track density and irradiation energy seems to be implicit in the low-energy data. The contrast between this result and that at the higher irradiation energies is due mainly to the difficulties of counting dense tracks as mentioned before. The appearance of low-energy autoradiographs is exemplified in Figure 16. Besides the lower track density, notice that many tracks exhibit a characteristic conical shape.

Diffusion Gradients

In conjunction with calibration experiments four and five, the diffusion couple 122867 was irradiated. Thus, autoradiographs

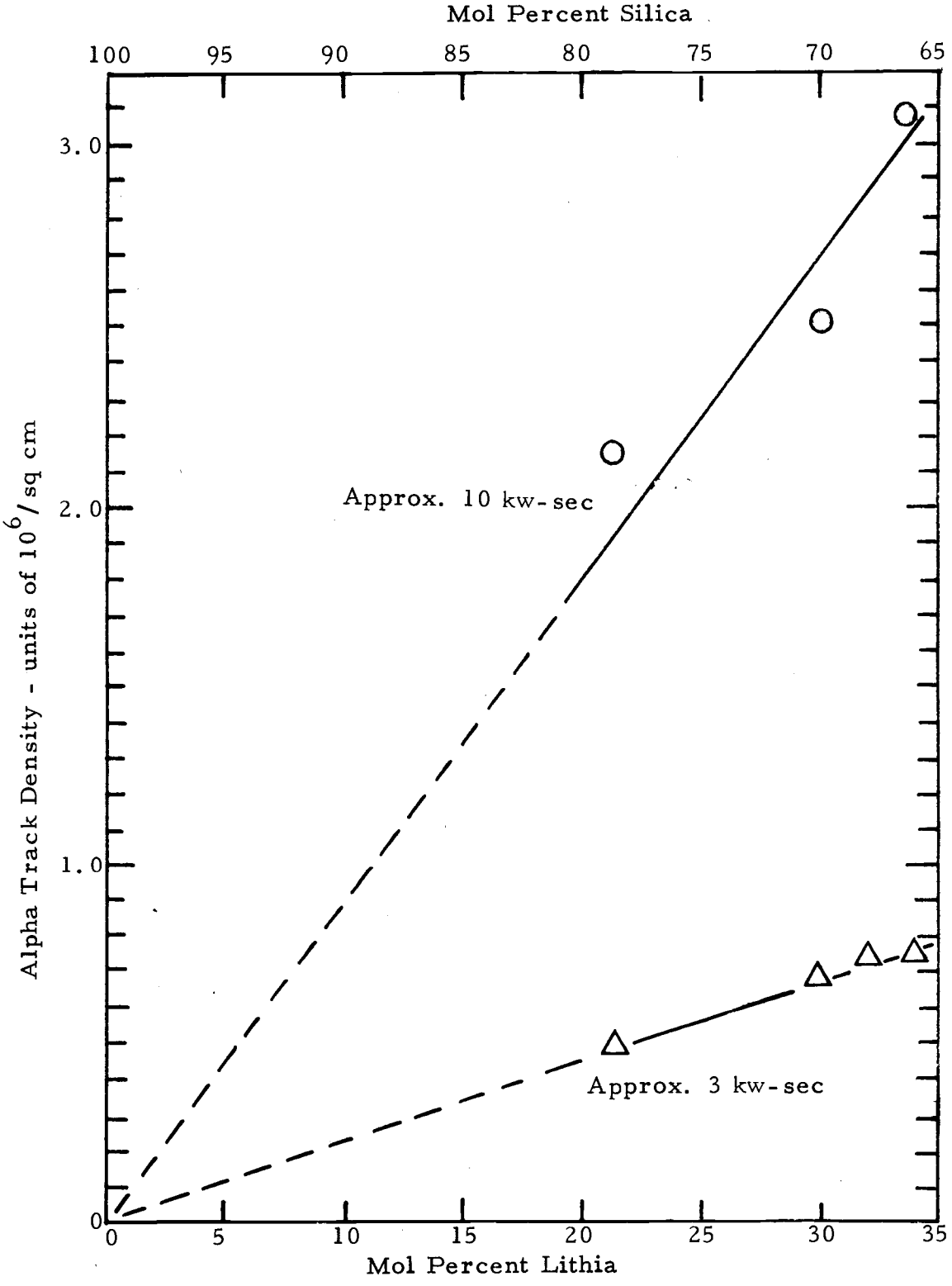

Figure 15. Composite calibration from experiments one, four and five,

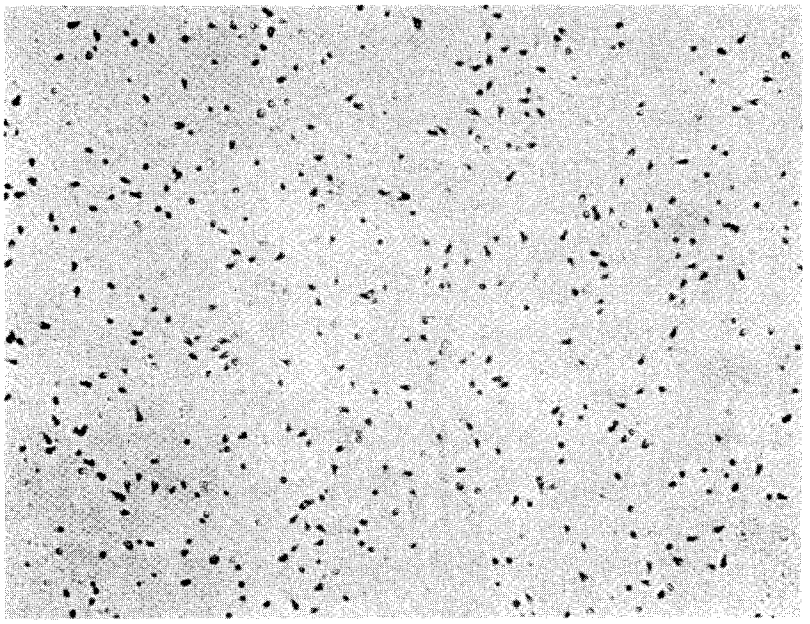

Figure 16. Etched alpha tracks in cellulose nitrate, resulting from 3 kw-sec irradiation of specimen H5 by thermal neutrons, with an apparent track density of about 8×10^5 per sq cm, magnified 400X.

1 22867 (4) and 1 22867 (5) were produced. In the first instance, the couple had been annealed for 186.4 hours, and in the second instance, the couple had been annealed for 350.3 hours. Throughout the diffusions, the temperature was between 855° and 910° C. Mosaic sequences of photographs were taken along radial diffusion directions. One sequence for 1 22867 (4) and two separate sequences for 1 22867 (5) were prepared. Each photo was divided into sections two cm wide for track counting, the two-cm dimension being in the diffusion direction. The glass overlay technique was used in counting tracks. Results are shown in Figures 17 and 18. Diffusion zones some 1,000 to 2,000 microns thick are evident. In comparison, autoradiographs of diffusion couples, before any diffusion, typically revealed abrupt changes of track densities corresponding to the interfaces between materials. Except in a few locations, the as-cast junctions appeared to be less than 20 microns thick, and part of this apparent thickness was due to the inevitably oblique paths of some alpha particles. The diffusion profiles are strongly suggestive of compositional heterogeneities, perhaps in the form of phase separations. This same impression, in two dimensions, often results from overall viewing of track photographs. Examine Figure 16 again, for example. The tracks commonly seem to be grouped in a way that presents a general pattern resembling a crystallite-structure pattern. Such observations are very superficial, but they are haunting nevertheless.

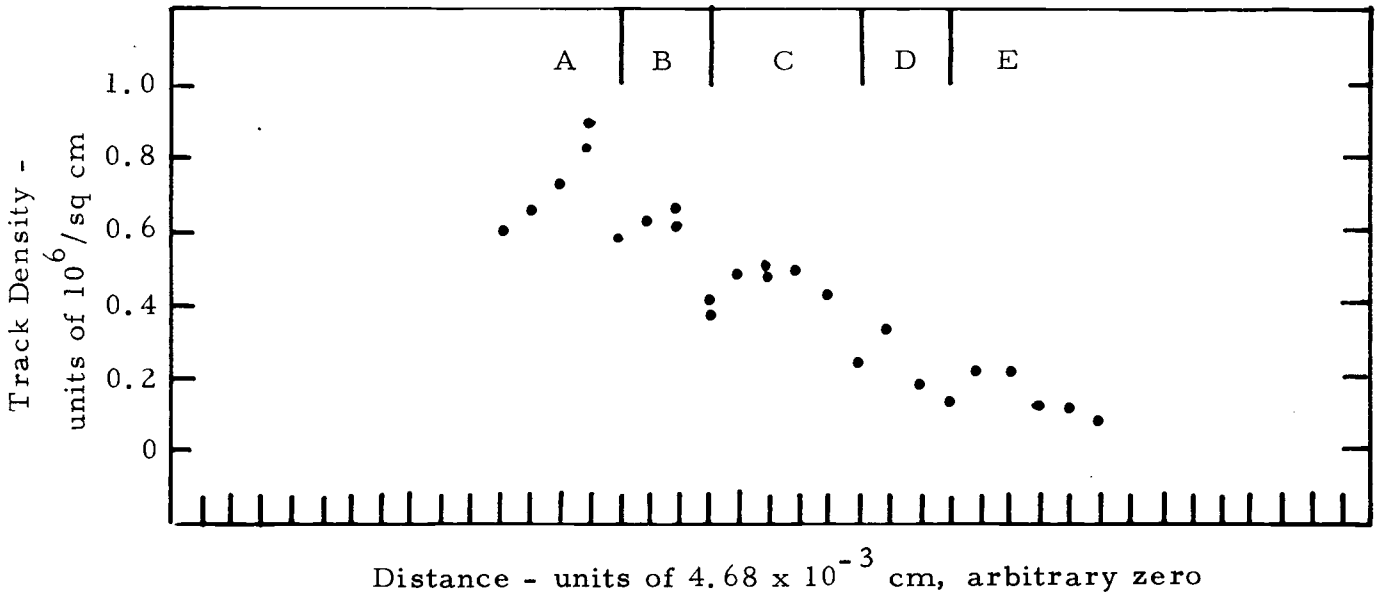

Figure 17. Diffusion zone profile 122867(4).

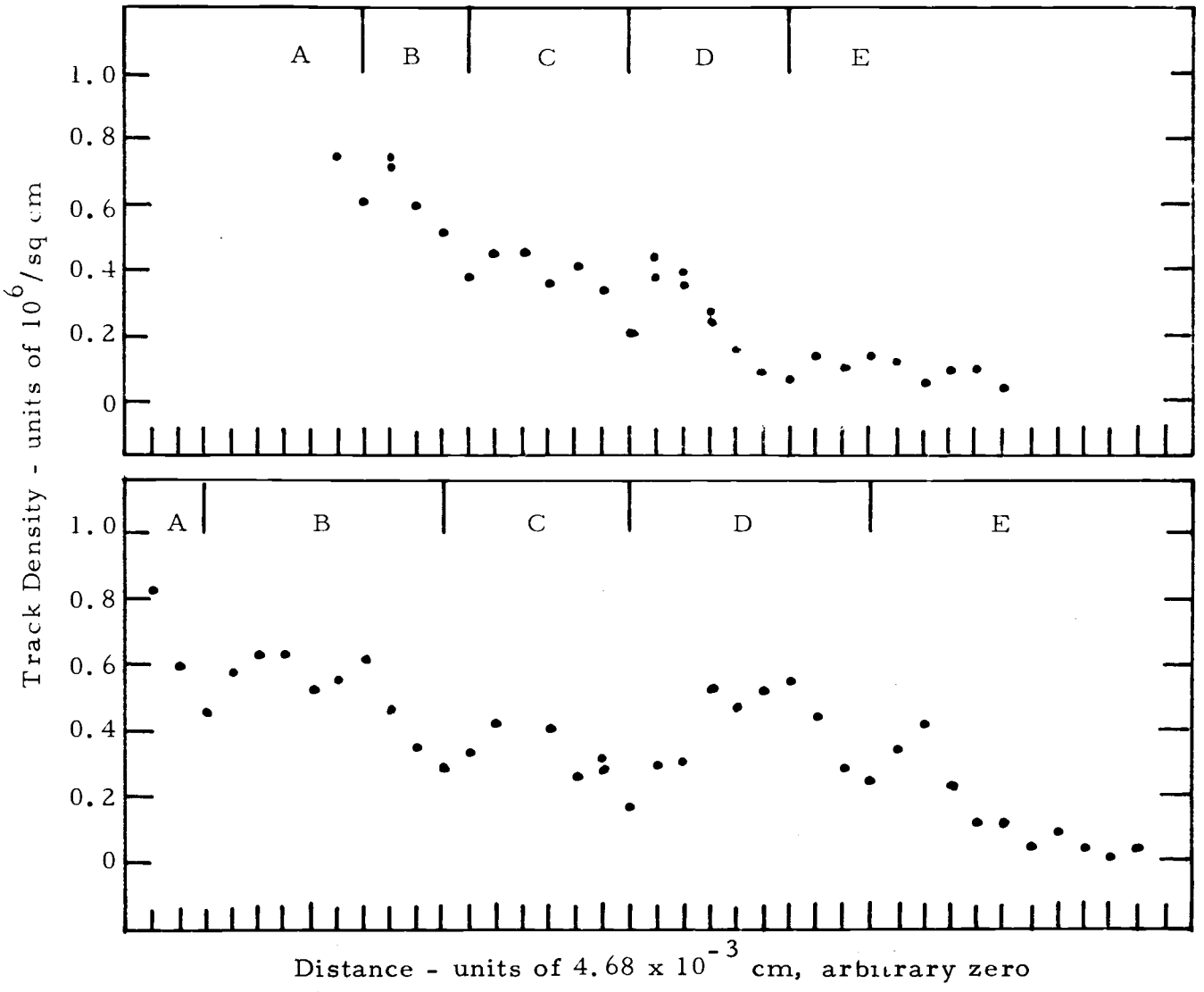

Figure 18. Diffusion zone profiles 122867(5).

INTERPRETATION AND DISCUSSION

A major observation agreed upon by most investigators of the lithia-silica system is that the solid-phase region between the disilicate and pure silica is characterized by heterogeneities. Beyond this, there is uncertainty and conjecture about both the nature and scale of the heterogeneities. Indeed, as apparent in the Introduction of this report, it is probable that the nature and scale vary according to thermochemical histories of individual specimens.

In diffusions near 885° C between H3 material (lithium disilicate) and vitreous silica, it should be possible to form the substances listed below in the order of decreasing lithium content:

1. devitrified $Li_2O \cdot 2SiO_2$;
2. $Li_2O \cdot 2SiO_2$ enriched in Si^{4+} and depleted in Li^+ by crystalline solution;
3. vitreous SiO_2 enriched in Li^+ or Li_2O by liquid miscibility;
4. vitreous SiO_2.

In fact, such a sequence of compositions would be quite consistent with the superficial appearance of couples after diffusion (see Figure 8). Although he wrote specifically about metals and metallic compounds, Rhines (28, p. 123-124) has stated an important principle governing well-behaved diffusions:

> The layers formed by the isothermal and isobaric diffusion... across an interface correspond in kind and in the order of occurrence to all regions in the phase diagram lying between the concentrations of the original bodies and having three or more degrees of freedom according to the phase rule (two or more degrees of freedom in the conventional temperature -- concentration section where pressure is disregarded).

This, of course, is just the Gibbs phase rule with special emphasis. It means that in binary systems, diffusion will yield smooth concentration gradients only in single-phase regions. If there are two-phase regions, they will cause discontinuities in the concentration gradient. In ternary diffusion systems, smooth concentration gradients will be obtained in both single-phase and two-phase regions, and three-phase regions will correspond to discontinuities. It is relevant also to note that the true driving force in diffusion is not a gradient or difference of concentration as such, but a gradient or difference of free energy or chemical potential. Thus, in complicated or multi-component systems, and especially in spinodal systems (5), concentration reversals are quite possible. Finally, separate single-phase regions of equilibrium systems cannot share a boundary -- they must be separated by two-phase regions.

Now, if the silica-lithium disilicate system can be treated as binary and if a sequence of phases similar to the list given above, but with appropriate intervening two-phase regions, is actually obtained by diffusion between the terminal constituents, the

concentration gradient should be characterized by relatively smoothly varying regions punctuated with discontinuities. These are general features that can be seen in Figures 17 and 18, but it is difficult and probably a mistake to try to apply the guidelines too rigorously or too specifically to these particular diffusion profiles. The presence of discontinuities fairly can be interpreted as evidence of mixed phases, but because of the highly metastable character of the system, boundaries of neither single- nor two-phase regions are inviolate. Neither is it clear exactly what constitutes a separate phase, except that crystalline material should be distinguished from vitreous matter. Phase regions are not strictly bounded, and a phase (or phase mixture) can readily overlap into a range of compositions that otherwise or elsewhere corresponds to mixed phases (or one phase). However, separate phase regions should tend to extend between some pair of metastable boundaries, even though intermediate boundaries are ignored. Thus, the really important diffusion-profile features are the appearance of phase separations and the recurrence of certain limiting compositions. A corresponding interpretation of the data is suggested as one possibility. In fact, it is possible to divide each of the profiles into five regions as indicated by the letters A through E on the figures. Then the range of variation within each region can be estimated, with the result shown in Table 3.

According to this analysis, the A regions would comprise the

devitrified lithium disilicate and its slightly modified crystalline solutions, and the remaining B, C, D, and E regions would be lithium-, or lithia-containing glasses. If this sort of conjecture is continued, it is most reasonable to assume that the apparent phase separations of the glasses result from the anticipated immiscibility. The basic mechanisms by which such phase separations occur are described well elsewhere (5). In the A regions, compositions down to about 25 mol percent lithia or less are found, but further reductions of lithia seem to cause instability because there is a reversion to higher compositions of about 30 mol percent in the B regions. The 25 and 30 mol percent compositions probably lie, at 885° C, near metastable extensions of the liquidus boundaries (see Figure 1) that meet at the eutectic isotherm to form the eutectic point. At the other end of the profiles, in the E regions, the first marked instability shows up at about 11 mol percent lithia, on the average, and the reversion is to about 7 mol percent. Then, in the B, C, and D regions, average compositions oscillate from about 10 and 15 mol percent on one hand to about 20 and 21 mol percent on the other hand. On this basis, the vitreous regions seem to be approximately from 0 to 7, 7 to 11, 11 to 15, 15 to 20, 20 to 25, and 25 to 30 mol percent lithia. In the latter of these regions, either a glass or crystalline solution appears permissible. Between 30 and 33 mol percent lithia, there is only the crystalline solution. By a final stretch of the imagination, it is

Table 3. Regional Variations of Lithia Composition in Diffusion Profiles

	Profile Identification			
	122867(4)	122867(5)A	122867(5)B	Average
Region A:				
minimum	(0.59) 26%	(0.61) 27%	(0.46) 20%	(0.55) 25%
Region B:				
maximum	(0.66) 29%	(0.75) 33%	(0.63) 28%	(0.68) 30%
minimum	(0.38) 16%	(0.38) 16%	(0.24) 11%	(0.33) 15%
Region C:				
maximum	(0.52) 24%	(0.45) 20%	(0.43) 20%	(0.47) 21%
minimum	(0.24) 11%	(0.21) 10%	(0.17) 8%	(0.21) 10%
Region D:				
maximum	(0.34) 15%	(0.45) 20%	(0.55) 25%	(0.45) 20%
minimum	(0.14) 6%	(0.08) 4%	(0.25) 11%	(0.16) 7%
Region E:				
maximum	(0.22) 10%	(0.15) 7%	(0.42) 20%	(0.26) 11%)

Note: Numbers in parentheses are track densities in units of 10^6 per sq cm. Percentages are mol percent of lithia based on the calibration in Figure 15.

suggested that 7 and 20 mol percent of lithia approximate points on the miscibility boundary at about 885° C, and that 11 and 15 mol percent of lithia are corresponding approximations of points on the spinodal boundary. These guesses were included in Figure 2 for comparison with other predictions and measurements. The agreement is not bad on the lithia-rich side of the miscibility gap, but on the silica-rich side, this investigation implies a narrower region of immiscibility than that predicted. It is probably no accident that some of the limiting compositions seem to be near the eutectic at 30 mol percent, the trisilicate at 25 mol percent, the tetrasilicate at 20 mol percent, and the pentasilicate at 16.7 mol percent lithia.

It would be presumptuous, on the basis of the results available, to claim that the foregoing explanation of observations is fact. It is a possible explanation, it fits in well as an extension of a growing pool of knowledge about the lithia-silica system, and it is compatible with the data on hand, but it is not deducible from that data with a high level of confidence. A basis for criticism is a suggestion that the regional variations of the diffusion profiles may not be statistically significant in view of uncertainties of the present autoradiographic technique. If the binomial approximation of a normal distribution is applied as a test at a 70 percent level of confidence, an individual determination must deviate from the mean determination by about 84 percent of the root mean value in order to be considered

significantly different. Now, the actual numbers of pits per incremental area, counted to obtain the diffusion profiles, ranged up to about 70. Therefore, consider the examples of 20, 40, and 60 counts. The corresponding significant deviations would be 17.5, 13.2, and 10.8 percent of the respective numbers of pits. Translated into track density units, the uncertainties at various values are as follows: $0.25 \pm 0.04 \times 10^6$, $0.50 \pm 0.06 \times 10^6$, and $0.70 \pm 0.08 \times 10^6$ tracks per sq cm. It is true that some of the peaks and valleys of the diffusion profiles seem to be contained within these limits, but several are not, indicating that at least some of the differences are probably real even against the binomial test.

Part of the data plotted in Figures 13 and 14 were based on tracks counted in partial sections of autoradiograph frames. The sectional areas and corresponding numbers of tracks were comparable to the same factors related to the diffusion profiles. So, means are available for a more accurate estimate of dispersion based on the usual formulation of standard deviation for small samples. Results of this computation are given in Table 4. Since a half-breadth equal to one standard deviation represents a confidence level of about 68 percent, a nearly direct comparison can be made with the binomial estimates at a 70 percent confidence level. In general, counting accuracy was slightly better than predicted by the binomial considerations. Consequently, the proposed interpretation of observations

becomes even more plausible.

Table 4. Track Counting Uncertainties

Tracks Counted		
Mean	Standard Deviation	Percentile Deviation
82	3.0	3.7%
73.6	8.1	11.0%
71.5	5.8	8.1%
67.5	7.1	10.6%
61	1.9	3.1%
58.8	7.8	13.3%
45	6.6	14.6%
41.6	5.2	12.4%
Typical Deviation - approx. 10%		

Note: Each sample represents five counts.

A third clue to the credibility of the data is implicit in the diffusion profiles of Figures 17 and 18 themselves. In obtaining the mosaic sequences of photographs, a certain amount of overlapping was essential in order to match photographs. Sometimes the overlap exceeded the width of a section ruled off for track counting, and the corresponding tracks were counted on each of the two photographs. This was the origin of the two data points plotted in certain places in the diffusion profiles. Of nine duplications, the one with the greatest percentage difference was observed in the D region of profile 122867(5)A, and it very nearly equaled the ten percent indicated as typical in Table 4.

The matter of counting statistics is important too in connection with attainable resolutions of compositional differences. If the

profile variations in Figures 17 and 18 can be accepted as real, it means that compositions were meaningfully resolved over distances of a few tens of microns. If those same variations are insignificant, useful resolutions were about an order of magnitude poorer.

If the apparent compositional variations of diffusion profiles are interpreted as normal fluctuations from a least-squares trend, it is equivalent to assuming that diffusion between silica and lithium disilicate glasses produces a smooth and continuous variation of intermediate compositions. Thus, if the system exhibits binary behavior, the diffusion zone would have to be of a single phase. This interpretation is untenable under the weight of most prior evidence concerning the phase system, and in view of the phase differences visually obvious (see Figure 8) in the diffused specimen studied in this investigation. An interpretation based on a heterogeneous model is clearly preferable.

CONCLUSIONS

Although many technical problems were encountered, and the meaning of information concerning the silica-lithium disilicate system is uncertain, original objectives were fulfilled in surprising degree. Relative to neutron-induced autoradiography:

1. Basic guidelines were established for immediate applications of certain types, and as a basis for further improvement of the technique.
2. The main problem areas were defined as inadequate control and monitoring of irradiation energy, inadequate control and reproducibility of the etching process, and the inaccuracies and tediousness of counting practices.
3. Interesting capabilities of the method were demonstrated for studying materials. The limit of compositional resolution in current technology is related to track counting difficulties through the minimum counting area necessary to provide statistically significant determinations.

Relative to the lithia-silica system:

1. The state of knowledge concerning the system was reviewed in a context not previously presented.
2. The problems of preparing and diffusing couples of materials in the system were clarified and solved well enough to obtain intermediate compositions, distributed suitably

for research purposes.

3. A tentative evaluation of the diffusion profiles as determined by neutron-induced autoradiography contains interesting implications about the immiscibility of both glasses and ceramics of the system. The positions of two points on the liquid miscibility boundary were estimated -- one on the lithia-rich side, the other on the silica-rich side. The former agrees generally with prior information, and the latter is apparently the first experimental evidence germane to the compositions richer in silica.
4. The essential soundness of the experimental approach was demonstrated, and groundwork was prepared for more accurate experiments to confirm or clarify the tentative results.

BIBLIOGRAPHY

1. Andreev, N. S. et al. Chemically heterogeneous structure of two-component sodium and lithium silicate glasses. In: The structure of glass. Vol. 3. Catalyzed crystallization of glass, ed. by E. A. Porai-Koshits et al., tr. by E. B. Uvarov. New York, Consultants Bureau, 1964. p. 47-52.

2. Aver'yanov, V. I. and E. A. Porai-Koshits. Electron microscopic investigation of heterogeneous structure and initial crystallization stages of glasses in the system Li_2O-SiO_2. In: The structure of glass. Vol. 5. Structural transformations in glasses at high temperatures, ed. by N. A. Toropov and E. A. Porai-Koshits, tr. by E. B. Uvarov. New York, Consultants Bureau, 1965. p. 63-81.

3. Benton, E. V. A study of charged particle tracks in cellulose nitrate. San Francisco, 1968. 228 p. (U. S. Naval Radiological Defense Laboratory. Report TR-68-14. Defense Documentation Center number AD 666543)

4. Bokin, P. Ya. et al. Mechanical properties and microstructure of lithium silicate glasses at different stages of crystallization. In: The structure of glass. Vol. 5. Structural transformations in glasses at high temperatures, ed. by N. A. Toropov and E. A. Porai-Koshits, tr. by E. B. Uvarov. New York, Consultants Bureau, 1965. p. 126-133.

5. Cahn, J. W. Spinodal decomposition. Transactions of the Metallurgical Society of the American Institute of Mining, Metallurgical and Petroleum Engineers 242:166-180. 1968.

6. Cahn, J. W. and R. J. Charles. The initial stages of phase separation in glasses. Physics and Chemistry of Glasses 6:181-191. Oct. 1965.

7. Chaklader, A. C. D. and A. L. Roberts. Transformation of quartz to cristobalite. Journal of the American Ceramic Society 44:35-41. 1961.

8. Charles, R. J. Activities in Li_2O-, Na_2O-, and K_2O-SiO_2 solutions. Journal of the American Ceramic Society 50:631-641. 1967.

9. Charles, R. J. Metastable liquid immiscibility in alkali metal oxide-silica systems. Journal of the American Ceramic Society 49:55-62. 1966.

10. Charles, R. J. Some structural and electrical properties of lithium silicate glasses. Journal of the American Ceramic Society 46:235-243. 1963.

11. Davies, J. H. and R. W. Darmitzel. Alpha autoradiographic technique for irradiated fuel. Nucleonics 23:86-87. July 1965.

12. Florinskaya, V. A. The study of the construction of glass by various physical methods. In: Fourth All-Union Conference on the Vitreous State, Leningrad, Izd-vo Nauka, 1964. p. 13-22. (U. S. Air Force. Foreign Technology Division. Translation FTD-HT-23-873-67)

13. Freiman, S. W. and L. L. Hench. Kinetics of crystallization in Li_2O-SiO_2 glasses. Journal of the American Ceramic Society 51:382-387. 1968.

14. Frondel, C. The system of mineralogy of James Dwight Dana and Edward Salisbury Dana. Vol. 3. Silica minerals. 7th ed. New York, Wiley, 1962. 334 p.

15. Glasser, F. P. Crystallization of lithium disilicate from Li_2O-SiO_2 glasses. Physics and Chemistry of Glasses 8:224-232. Dec. 1967.

16. Goganov, D. A. and E. A. Porai-Koshits. Investigation of the chemically heterogeneous structure of certain silicate glasses by the small angle x-ray scattering method. In: The structure of glass. Vol. 5. Structural transformations in glasses at high temperatures, ed. by N. A. Toropov and E. A. Porai-Koshits, tr. by E. B. Uvarov. New York, Consultants Bureau, 1965. p. 82-89.

17. Goganov, D. A., E. A. Porai-Koshits and Yu. G. Sokolov. Detection and study of very small heterogeneities with the aid of a new low-angle x-ray apparatus. In: The structure of glass. Vol. 3. Catalyzed crystallization of glass, ed. by E. A. Porai-Koshits, et al., tr. by E. B. Uvarov. New York, Consultants Bureau, 1964. p. 45-46.

18. Haas, L. A. and S. E. Khalafalla. Effect of physical parameters on the reaction of graphite with silica in vacuum. Washington, D. C., 1968. 21 p. (U. S. Bureau of Mines. Report of Investigations 7207)

19. Harris, H. M., J. E. Kelley and H. J. Kelly. Devitrification of a lithium disilicate glass. Washington, D. C., 1965. 14 p. (U. S. Bureau of Mines. Report of Investigations 6711)

20. Hurlbut, C. S., Jr. Dana's manual of mineralogy. 16th ed. New York, Wiley, 1956. 530 p.

21. Kalinina, A. M. et al. Crystallization products of lithium silicate glasses. In: The structure of glass. Vol. 3. Catalyzed crystallization of glasses, ed. E. A. Porai-Koshits et al., tr. by E. B. Uvarov. New York, Consultants Bureau, 1964, p. 53-64.

22. Korelova, A. I., M. G. Degen and O. S. Alekseeva. Microstructure of two-component lithium silicate glasses at various crystallization stages. In: The structure of glass. Vol. 3. Catalyzed crystallization of glass, ed. by E. A. Porai-Koshits et al., tr. by E. B. Uvarov. New York, Consultants Bureau, 1964. p. 65-68.

23. Kostanyan, K. A. and E. A. Erznkyan. Electrical conductivity of glasses of the system Li_2O-SiO_2 in the molten state. Armenian Chemical Journal 20:358-365. 1967.

24. Kracek, F. C. The binary system Li_2O-SiO_2. Journal of Physical Chemistry 34:2641-2650. 1930.

25. Liebau, F. Untersuchungen an Schichtsilikaten des Formeltyps $A_m(Si_2O_5)_n$. I. Die Kristallstruktur der Zimmertemperaturform des $Li_2Si_2O_5$. Acta Crystallographia 14:389-395. 1961.

26. Moriya, Y., D. H. Warrington and R. W. Douglas. A study of metastable liquid-liquid immiscibility in some binary and ternary alkali silicate glasses. Physics and Chemistry of Glasses 8:19-25. Feb. 1967.

27. Paige, J. I., H. M. Harris and H. J. Kelly. Devitrification of vacuum-melted glasses of the lithium metasilicate-silica compositional series. Washington, D. C., 1965. 15 p. (U. S. Bureau of Mines, Report of Investigations 6651)

28. Rhines, F.N. Diffusion coatings on metals. In: Surface treatment of metals. Metals Park, Ohio. American Society for Metals, 1941. p. 122-165.

29. Rindone, G.E. Further studies of the crystallization of a lithium silicate glass. Journal of the American Ceramic Society 45:7-12. 1962.

30. Roy, R. Metastable liquid immiscibility and subsolidus nucleation. Journal of the American Ceramic Society 43:670-671. 1960.

31. Shmeleva, N.A. and N.M. Ivanova. Lithium glasses and some of their crystallization characteristics. In: The structure of glass. Vol. 3. Catalyzed crystallization of glass, ed. by E.A. Porai-Koshits et al., tr. by E.B. Uvarov. New York, Consultants Bureau, 1964. p. 69-73.

32. Sosman, R.B. The phases of silica. Bulletin of the American Ceramic Society 43:213. 1964.

33. Sosman, R.B. The phases of silica. New Brunswick, New Jersey, Rutgers University Press, 1965. 388 p.

34. Vaisfeld, N.M. and V.I Shelyubskii. Electron microscope investigation of microcrystallization of glasses. In: The structure of glass. Vol. 3. Catalyzed crystallization of glass, ed. by E.A. Porai-Koshits et al., tr. by E.B. Uvarov. New York, Consultants Bureau, 1964. p. 37-42.